STARS

Electronic Theses and Dissertations, 2020-

2020

Novel Fibers and Components for Space Division Multiplexing Technologies

Juan Carlos Alvarado Zacarias
University of Central Florida

University of Central Florida

STARS
Showcase of Text, Archives, Research & Scholarship

NOVEL FIBERS AND COMPONENTS FOR SPACE DIVISION MULTIPLEXING
TECHNOLOGIES

by

JUAN CARLOS ALVARADO ZACARIAS
B.S. Physics, Veracruzana University, 2013
M.S. Optics, National Institute of Astrophysics, Optics and Electronics, 2015
M.S. Optics and Photonics, University of Central Florida, 2020

A dissertation submitted in partial fulfilment of the requirements
for the degree of Doctor of Philosophy
in the College of Optics and Photonics
at the University of Central Florida

Fall Term
2020

Major Professor: Rodrigo Amezcua-Correa

ABSTRACT

Passive devices and amplifiers for space division multiplexing are key components for future deployment of this technology and for the development of new applications exploring the spatial diversity of light. Some important devices include photonic lantern (PL) mode multiplexers supporting several modes, fan-in/fan-out (FIFO) devices for multicore fibers (MCFs), and multimode amplifiers capable of amplifying several modes with low differential modal gain penalty. All these components are required to overcome the capacity limit of single mode fiber (SMF) communication systems, driven by the growing data capacity demand.

In this dissertation I propose and develop different passive components and amplifiers for space division multiplexing technologies, including PL mode multiplexers with low insertion loss and low mode dependent loss to excite different number of modes into few mode fibers (FMFs). I demonstrate a PL with a graded index core that better matches the mode profiles of a graded index FMF supporting six spatial modes with mode dependent loss (MDL) ranging from 2- to 3-dB over the entire C-band. Multicore fibers can alleviate the capacity limit of single mode fibers by placing multiple single mode cores within the same fiber cladding. However, interfacing single mode fibers to MCFs can be challenging due to physical limitations, in this dissertation I develop and fabricate different types of FIFO devices to couple light into MCFs with high efficiency and having up to 19 cores. I demonstrate high coupling efficiency with insertion loss below 0.5 dB per FIFO into a 4-core MCF and below 1 dB for a 19-core MCF. Multimode erbium doped fiber (EDF) amplifiers are required to amplify each mode within the few mode transmission fiber, the main challenge is to provide an amplifier with low differential modal gain, in this dissertation I present the first coupled-core amplifier concept compatible with FMFs. A 6-core coupled-core EDF can be spliced with low insertion and low MDL to a FMF supporting 6 spatial modes via a slight taper transition. The amplifier introduces 1.8 MDL with gain variation over the entire C-band below 1-dB.

ACKNOWLEDGMENTS

TABLE OF CONTENTS

LIST OF FIGURES

LIST OF TABLES

CHAPTER 1: INTRODUCTION

Motivation

The data traffic over the last few years has been increasing at a constant rate, this has lead to single mode fibers (SMFs) to be pushed to the limit of their transmission capacity. New technologies and approaches have been proposed to overcome this issue, including new fibers such as multicore fibers (MCFs), few mode fibers (FMFs) and coupled-core fibers (CCFs) that can exploit the spatial degree of freedom for data transmission, together with new modulation formats to enable higher data transmission.

New emerging applications and the exponential grow of bandwidth demand have pushed single mode fibers (SMFs) close to the edge of its transmission capacity, new technologies need to be developed to scale with the growing data transmission demand.

There are different degrees of freedom from which we can scale the data transmission through optical fibers, including time, quadrature, frequency, polarization and space. Of these degrees of freedom, space is the one that has not been completely researched and thus, it is the scope of this dissertation to propose new components that can be integrated into future space division multiplexing (SDM) systems including mode multiplexers and amplifiers with relatively good performance.

Different approaches exist when it comes to SDM technologies, one is the use of different modes as transmission channels in few mode fibers (FMFs), another one is the use of multicore fibers where each core supports only the fundamental mode, the third approach combines both of these approaches resulting in a few-mode multicore fiber where different cores in a single cladding support a certain number of modes. However, these technologies have their limitations as in a FMF, different modes travel a different speeds broadening the impulse response as the light propagates

1

down the fiber, making it difficult for digital signal processing (DSP) to recover the original information. In the case of multicore fibers one of the main impediments is the crosstalk that occurs between cores and that increases with the fiber length. It is very difficult to establish which one of the proposed technologies is the one with the best performance, but certainly, research on this area can pave the basis to the understanding and improvement of the aforementioned technologies.

Passive component and amplifiers are key elements on the integration of SDM technologies as they represent the metrics on which SDM stands. Mode multiplexers (MUX) and de-multiplexers (DEMUX) are required to access different channels of new proposed transmission fibers supporting few modes while providing low insertion loss (IL) and low mode dependent loss (MDL) to transmission fibers. On the other hand, few mode and multicore amplifiers with good performance over the telecommunication C-band are required to compensate for the loss that inherently occurs as the light travels through the fiber.

Optical fibers

An optical fiber is an optical waveguide with a cylindrical core surrounded by a cylindrical cladding whose refractive index is lower than that of the core ($n_1 > n_2$). If the change in refractive index is abrupt we have a step index fiber, whereas if the refractive index decreases gradually inside the core, the fiber is called graded index. In practice fibers can support many different modes depending on the characteristics of the fiber itself. A fiber is described by parameters such as the core size, refractive index profile and the wavelength at which the fiber is used. By increasing the core size, the number of supported modes increases. The number of modes for a given fiber with a step index profile is defined as[1]

$$V = \frac{2\pi}{\lambda}\sqrt{n_1^2 - n_2^2} \tag{1.1}$$

where λ is the wavelength and a is the radius of the fiber core. A fiber is single-mode when only supports one spatial mode, also known as the fundamental mode or linearly polarized LP_01. The cutoff condition for other supported modes is also determined by the V parameter of the fiber. When $V = 2.405$, the fiber only supports the fundamental mode and for $V > 2.405$ the fiber supports more modes as the V number increases.

Fiber tapering analysis

Fiber tapers have been studied for different applications, in this dissertation I present different devices that are based on tapering multiple fibers together, for this is very important to realize what it actually implies having a fiber taper. A taper fiber transforms the mode of a given fiber into a cladding mode at the tapered end of the fiber, if the taper is done gradually and the adiabaticity criteria is met, the light from the fiber core gets couple into the fiber cladding as shown in Fig. 1.1 where the mode slowly moves from the core into the cladding. A taper is adiabatic if the taper angle is small enough to prevent power loss from the fundamental mode as it propagates along the taper length. Considering a local taper length-scale z_t at a given taper angle defined as $\Omega(z) = \arctan|\frac{d\rho}{dz}|$ where z is the distance along the taper and $\rho = \rho(z)$ is the local core radius. In practice if $\Omega(z) << 1$, then [2]

$$z_t \approx \frac{\rho}{\Omega} \tag{1.2}$$

The coupling length between the two modes is the bet length $z_b = z_b(z)$ between the fundamental

3

propagated mode and the second local modes, where

$$z_b = \frac{2\pi}{\beta_1 - \beta_2} \tag{1.3}$$

and $\beta_1(z)$ and $\beta_2(z)$ are the respective propagation constants. One can now analyze the case for $z_t \gg z_b$ along the taper, negligible coupling will occur to second local modes and the fundamental mode will propagate with negligible loss. IF $z_t \ll z_b$ there is significant coupling to the second local mode and the taper will not be adiabatic. The condition for $z_t = z_b$ provides the boundary between adiabatic and lossy tapers. The condition is given by

$$\Omega = \frac{\rho(\beta_1 - \beta_2)}{2\pi} \tag{1.4}$$
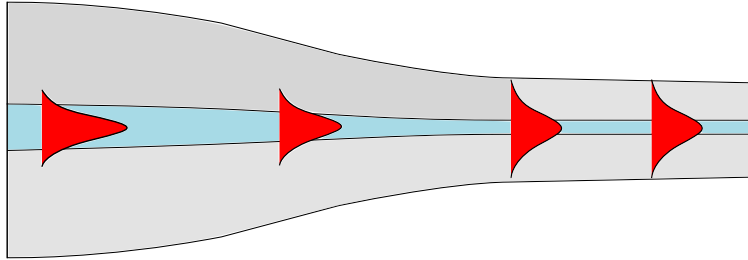
Figure 1.1: Schematic of a fiber taper, at the beginning the light is confined within the fiber core and after the taper, the light fills up the fiber cladding.

Starting from a single mode fiber, supporting only one single mode at a given wavelength, one can use a heat source and stretch the fiber while is heated up by the source. After a specific point along the tapering transition, the light will start to leak out of the core into the cladding, if we continue and make the fiber even smaller, the light is no longer confined in the core. Now imaging that the fiber is surrounded with a material having a lower refractive index than silica, in that case, the light radiates out of the core along the taper but if the taper is done adiabatically, all the light will

be captured by the secondary material that surrounds the initial fiber, in other words, there is a mode conversion from one single mode fiber into another single mode fiber which characteristics are given by the index contrast with the low refractive index material and the final core size after tapering. will have created a mode converter going form a single mode fiber to another single mode fiber with a different mode field diameter (MFD) given by the refractive index contrast of the secondary material.

Now lets examine the case of two SMFs, if we surround these fibers with a secondary material with a lower refractive index and analyse what happens during the taper, we see that at some point during the transition the light propagating within each core starts to couple to the other fiber and at the end we have created a new multimode waveguide where the number of modes is the same as the number of initial fibers there are in the beginning. This idea can be extended to multiple number of fibers surrounded by a lower refractive index material and then tapered meeting the adiabaticity criteria for obtaining a new multimode waveguide in the tapered end. Fiber tapers are widely use for different applications including change of mode size or shape, evanescent field interactions, fused couplers, mode coupling, among others. In this dissertation I present different applications of fiber tapers for space division multiplexing technologies.

Fibers for space division multiplexing

Single mode fibers have been widely used for high capacity long distance transmission over the last three decades, SMFs provide low loss and large bandwidth for data transmission. SMF cables can hold thousands of this fibers to increase the data capacity per cable. However, new fiber types are required for increasing the data transmission in the coming years as SMF reach its capacity limit. When it comes to SDM, different approaches can be taken, if we think of increasing the data capacity carried out by a single fiber, many options are available and it is still unclear which one

will finally replace SMF transmission in the future. Multiplicity of cores in a multicore fiber can be considered space division multiplexing as the number of cores increases within the same fiber cladding, each core carries out the information as a typical SMF will do over a specific distance. In the case of few mode fibers, modes are used as transmission channels over the fiber, while few-mode multicore fibers combine multiple cores with each core supporting multiple modes for data transmission.

Multicore Fibers

Multicore fibers (MCF) consist of multiple single mode cores arranged within the same fiber cladding, this fibers are limited by the core density, only certain number of cores can be placed in a standard 125 μm and the distance between the cores determines the amount of crosstalk with the neighboring cores, although these fibers can be engineered to reduce crosstalk by adding a trench around the cores. MCFs supporting more than 30 cores have been demonstrated [3] but an increased cladding diameter makes the fiber more susceptible to breaks. MCF require a special type of coupler to access each of the cores separately, and also require special splicers that are able to rotationally align each of the cores. These fiber types have the advantage of being similar in properties to existing SMFs and thus can take advantage of existent SMF components. One of the drawbacks of this fiber technology is the need of multicore fiber amplifiers able to equally amplify each mode within the MCF. Different MCF amplifiers have been proposed including a 7-core MCF amplifier [4], a reduced-cladding EDF bundle [5] and high density MCF amplifier with 32-cores [6].

Few mode fibers

Few mode fibers (FMF) support more tan one mode, consisting of a fiber with enlarged core o higher refractive index compared to SMFs. FMFs offer another degree of freedom for data transmission using the fiber modes as communication channels. Different types of FMFs have been proposed for data transmission including step index, graded index and ring core type fibers. FMFs are designed to reduce the reduce the group delay difference between the fiber modes so that transmission over several kilometers is possible. Different FMFs have been reported aiming to reduce the group delay and with different modes [7, 8]. Few mode and multimode fibers can be used for long distance transmission or short reach interconnects, depending on the fiber design and characteristics can be used for one or the other.

Few mode multicore fibers

In the case of few mode multicore fibers (FM-MCF), the idea is to combine the two previously discussed fiber types. FM-MCF consist of an arrange of cores with each one supporting more than one mode for data transmission, fibers with up to 36 cores supporting three spatial modes each one have been demonstrated [9]. These fiber types provide with high density data transmission but require complex mode multiplexers to send and receive data throughout the fiber with the addition of digital signal processing to recover the information.

Thesis overview

This dissertation discusses in chapter 2 the fabrication and characterization of photonic lanterns as mode multiplexer (MUX) and de-multiplexer (DEMUX) with mode selectivity and low mode dependent loss (MDL) for few mode fiber transmission and their scalability to higher number of modes/cores leading up to photonic lantern structures with 7 cores supporting six modes each one, for a high spatial density photonic lantern mode multiplexer.

Chapter 3 introduces the concept of fan-in/fan-out devices for coupling light into multicore fibers with high efficiency and low crosstalk, these devices and their performance can provide a solution to the increase in data transmission using MCFs where multiple single mode cores are confined within the same cladding, providing similar loss per channel compared to SMFs making them attractive for increasing the data transmission without complex digital signal processing for recovering the transmitted data.

In chapter 4 the concept of multimode amplifier is studied, in this chapter I propose and analyze a coupled core amplifier concept for few mode fiber transmission, able to reduce the differential modal gain and increase the mode mixing within the few mode fiber. The amplifier provides an average gain of more than 20-dB per channel.

Chapter 5 presents the fabrication and characterization of a multimode amplifier supporting 45 spatial modes using digital holography to evaluate each assembly step, measuring the transfer matrix at each splice point provides instant feedback on the amplifier performance and can be used to track the mode dependent loss and crosstalk of the amplifier.

CHAPTER 2: MODE SELECTIVE PHOTONIC LANTERNS FOR SPACE DIVISION MULTIPLEXING

Introduction

Recently, new alternatives to overcome the capacity limit of a single mode fiber (SMF) have been explored,including few mode fibers (FMFs) and multicore fibers (MCFs) [10]. Space division multiplexing (SDM) has emerged as an attractive solution to support future exponential growth in data traffic [11]. One of the key components for FMF transmission are the spatial multiplexer (SMUX) and demultiplexer (SDeMUX), photonic lanterns (PLs) are now considered as one of the most versatile mode multiplexers, they can provide low insertion loss, low mode dependent loss (MDL) and can work over a broad bandwidth [12, 13, 14, 15]. One of the main requirements of a PL is to have low loss to be used in a transmission link, including low MDL, low insertion loss and low modal crosstalk.

Mode multiplexers based on different technologies have been investigated including phase plates[16], multi-plane light conversion[17, 18, 19] and 3-D waveguides[20], however, mode multiplexers with low insertion loss (IL) and mode dependent loss(MDL) supporting higher number of modes with low modal crosstalk are still to be realized. PLs supporting 3, 6, 10, and 15 modes have been demonstrated[12, 13, 14, 15] and used in different transmission experiments in recent years[21, 22, 23, 24, 25]. PLs are now considered as one of the most versatile mode multiplexers as they can be fabricated with low loss and working over a broad bandwidth including C+L communication bands.
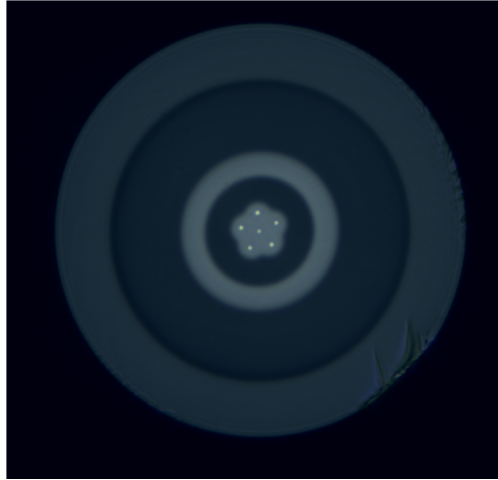
Figure 2.1: Microscope image of the fabricated photonic lantern

Step index photonic lanterns

Step index PLs were the first approach to an all-fiber mode multiplexer, it comprises a set of input fibers inserted into a low refractive index capillary that is adiabatically tapered to a multimode fiber waveguide that supports the same amount of modes as input fibers. To obtain mode selective photonic lanterns(MSPLs) one can choose the input fibers to have dissimilar cores, the number of dissimilar cores can be match to the number of mode groups in the PL.

Design and fabrication

We propose the fabrication of PLs supporting six spatial modes compatible with step index few mode fibers (FMFs) for SDM applications. The PLs can be optimized by choosing the right input fibers and by defining the taper length over which the modes are formed in the waveguide.

The MSPL is fabricated by inserting 6 graded index fibers with core/cladding diameters of 23.3/125 x1, 20.8/125 x2, 18.3/125 x2 and 14.5/86 into a low refractive index capillary with 345 μm inner
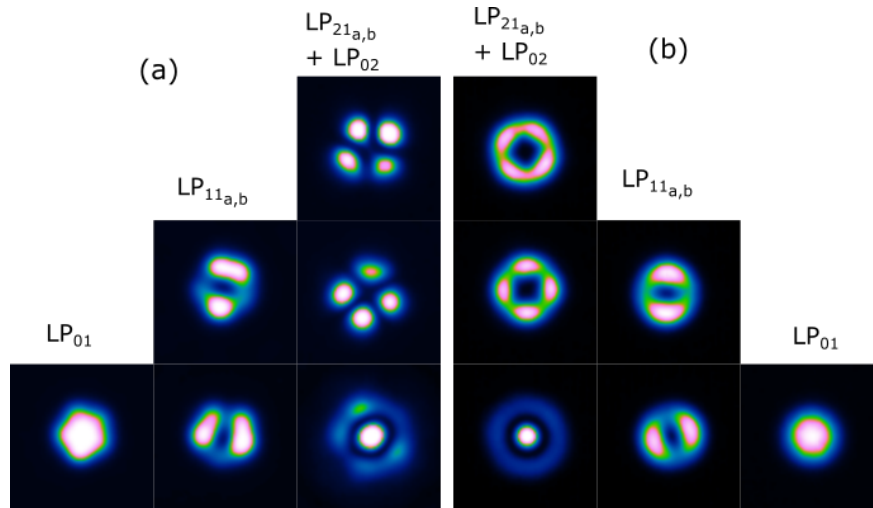
Figure 2.2: Near field mode profiles at a) the PL facet and b) after 5m propagation over step index FMF.

diameter and 830 μm outer diameter, enough to fit the six GI fibers in a tight package, the capillary has an index contrast of -19.5 $\times 10^{-3}$. The taper process is carried out in a glass processing machine in 3 different steps. In the first step, the capillary is tapered down to 330 μm and is inserted again into a second piece of the same capillary, in a second taper the new capillary is down tapered to 400 μm and in a final step, the MSPL is tapered to 120 um final outer diameter. The photonic lantern is characterized by measuring the mode profiles in the near field before and after splicing to a 5 m long piece of FMF supporting 6 spatial modes. Fig. 2.1 shows the cross section of the fabricated photonic lantern, the cladding diameter of the PL is 120 μm and the core diameter is 16 μm, one can observe the silica ring between the 2 fluorine-doped regions, notice that this silica ring comes from the first taper as the PL is tapered and inserted again in the same capillary tube. Inserting the PL into the same tube provides more material to the final PL cladding size, making it very close in outer diameter to the FMF which makes it easier for cleaving and splicing compared to having a PL with a smaller cladding diameter which usually increases the error during splicing leading to an increase of MDL and IL due to offset splice errors.

11
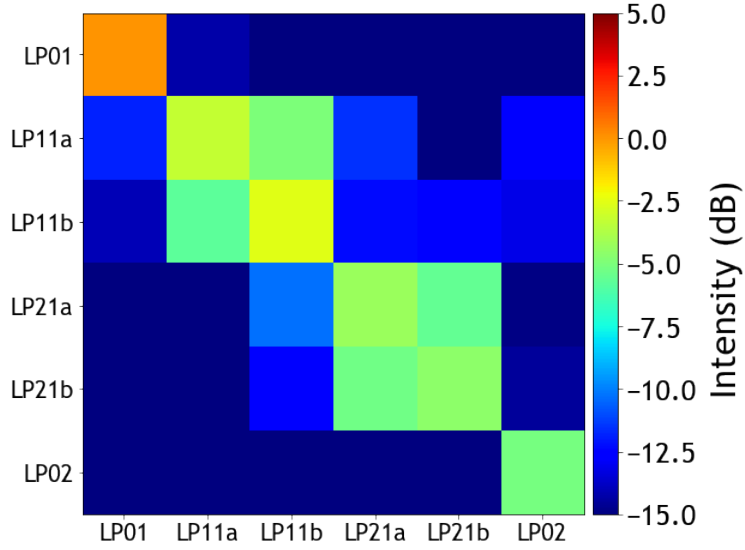
Figure 2.3: Measured transfer matrix for a pair of photonic lanterns spliced to step index FMF.

Characterization and results

In order to characterize the PL we obtain the near-field mode profiles at the lantern output and after splicing to the FMF as shown in Fig. 2.2, we observe that the modes after propagation in the FMF have low crosstalk as seen from the deep nulls in the higher order modes. A more detailed characterization is carried out by using a swept-wavelength interferometer with spatial diversity to obtain the transfer matrix (TM) of the PL, from the TM one can compute the mode dependent loss (MDL) of the device under test[26].

Fig. 2.3 shows the measured transfer matrix for a pair of PL multiplexers, we can clearly see the high mode selectivity of the device, crosstalk is observed within the same mode group and low modal crosstalk is observed overall. The low modal-crosstalk is a good indicator that the PL is able to excite the exact number of modes in the FMF.

Fig. 2.4 (a) shows the measured MDL obtained from the TM over a wide bandwidth that includes
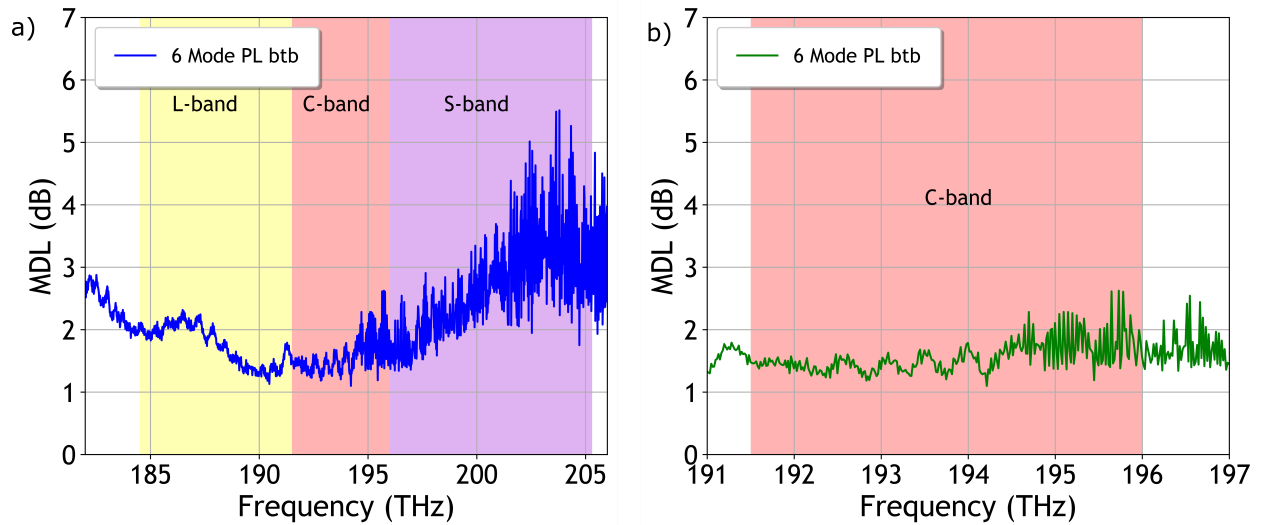
Figure 2.4: a) Measured MDL for a pair of photonic lanterns spliced to FMF over a long bandwidth that includes S+C+L transmission bands. b) Close up showing the MDL over the C-band with a very flat performance.

S+C+L communication bands, we see that the MDL of the PL over the C-band (see Fig. 2.4 (b)) is very low ranging from 1.1-dB to 2.6-dB with an average of 1.6-dB over the C-band, this value is for a pair of PLs, meaning that each lantern has an MDL of 0.8-dB over the C-band. This is the lowest MDL reported for a pair of six mode PL multiplexers. There is only little degradation of performance over the L-band as the MDL increases to over 2-dB showing that the PL can be used in both C+L communication bands. On the other hand, over the S-band we see that the variation of MDL is bigger an increases to over 5-dB at shorter wavelengths, this may be due to the fact that both the FMF and PL support more modes as the wavelength decreases, making it not optimum for this region.

Optimization of the PL making process can further reduce the MDL over shorter wavelengths, one way of doing this is by choosing a fluorine-doped capillary with a different index contrast so that the modes in the PL match the modes in the FMF.
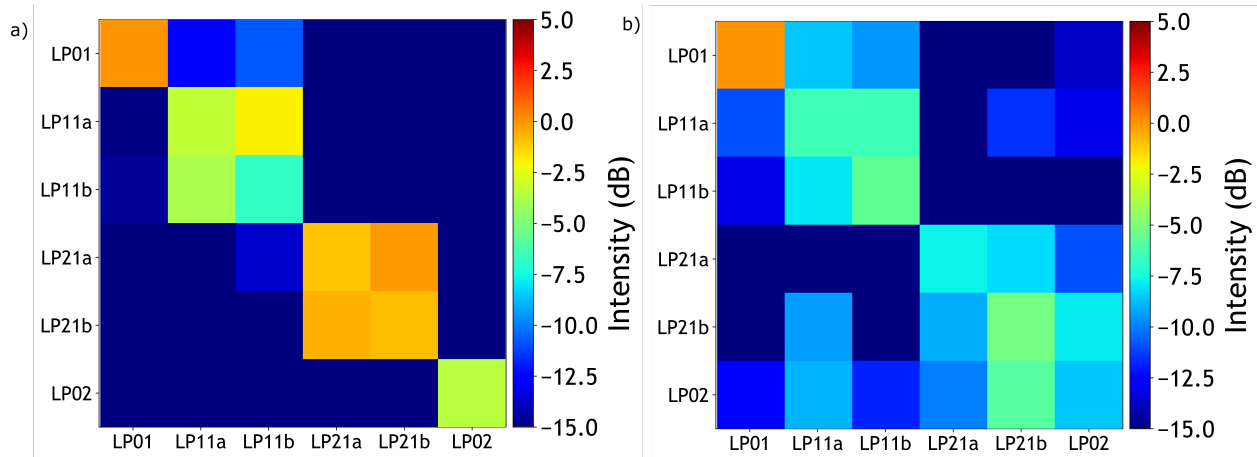
Figure 2.5: a) Measured TM at the output facet of the PL. b) Measured TM for a pair of photonic lanterns spliced to graded index FMF

In the case of graded index few mode fibers (GI-FMF) it is possible to excite the modes in the fiber using the same PL approach, even if the modes are not the same due to differences in the mode shapes at the output of the PL and the GI-FMF, one can fabricate the PL trying to reduce the MDL and insertion loss by choosing the right input fibers and index contrast for the low refractive index capillary. We measured the performance for the case when the PL is spliced to a 6-mode GI-FMF. Fig. 2.5 (a) shows the TM at the output of the PL, we can clearly see 4 mode groups with high selectivity, there is only crosstalk observed between the LP01 and LP11 modes. After splicing to the GI-FMF we see the degradation of mode selectivity (Fig. 2.5 (b)), more crosstalk is observed between groups, this is due to the mode overlap between the PL and the GI-FMF, where even if the MDL does not significantly change as shown in we see that the modes scramble in the GI-FMF and further optimizations are needed to overcome this issue.

The measured MDL at the output of the PL is measured using the same swept wavelength interferometer with spatial diversity operated in reflection mode where the light reflected from the cleaved facet of the PL is detected. This measurement only requires one single device. Fig. 2.6 (a) shows

14
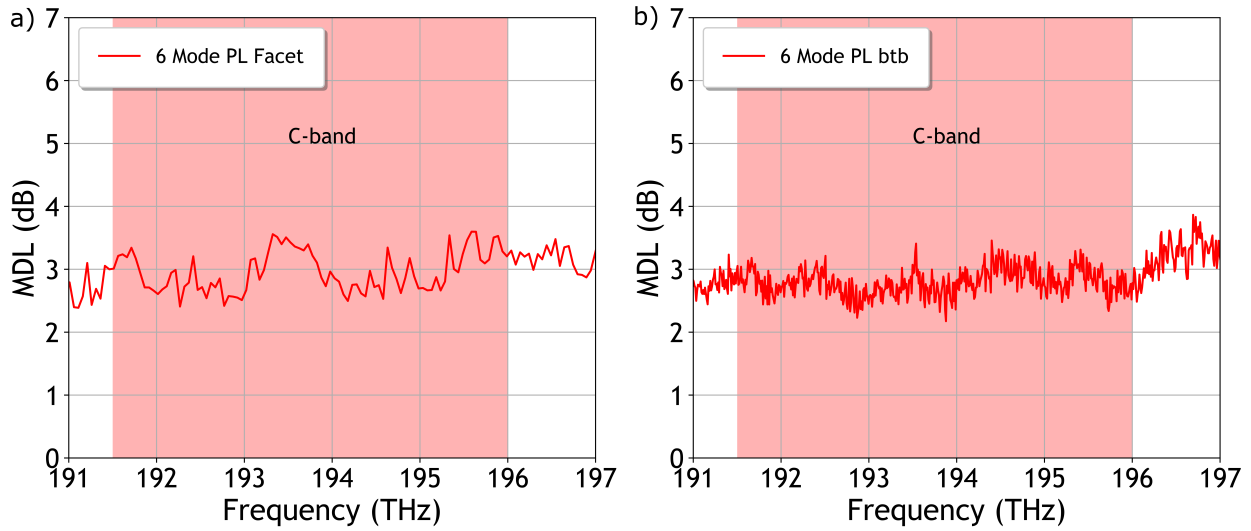
Figure 2.6: a) Measured MDL over the C-band for a) photonic lantern output facet, and b) pair of photonic lanterns spliced to GI-FMF.

the MDL measured over the C-band ranging from 2.5-dB to 3.5-dB, the MDL of the device is half of these values as we are measuring in reflection mode and the light travels twice over the device under test before it is detected. Thus, and MDL value between 1.3-dB and 1.8-dB is measured at the output of the PL. One can also notice the high selectivity of the PL, from the TM we see that each input fiber evolves into an specific mode at the end of the taper In Fig. 2.6 (b) we see the measured MDL over the C-band for pair of PLs after splicing to a 5-meters long piece of GI-FMF at the output of each PL. We see no degradation of the MDL over the C-band compared to the MDL value at the output of the PL, however, there is an increase in the modal crosstalk due to a mismatch in the mode sizes and/or a possible offset during the splicing of the PL and the GI-FMF.

15

Graded index photonic lantern

The design of PLs that better matches the properties of a FMF is of great importance for long-haul transmission as GI-FMF are required to provide low differential group delay (DGD) for easing the digital signal processing (DSP) because the modes do not scramble as much after traveling over long distance in the fiber. PLs can be scaled to a larger number of modes with the advantage that they can be easily splice to a transmission fiber [12, 14, 13, 15]. Unfortunately, as seen shown before previous PLs have a step index refractive index profile whose modes are slightly different than the modes of the typical graded index transmission fiber. This causes additional losses and crosstalk at the splice point between the PL and the transmission fiber making them not suitable for transmission over GI-FMF.
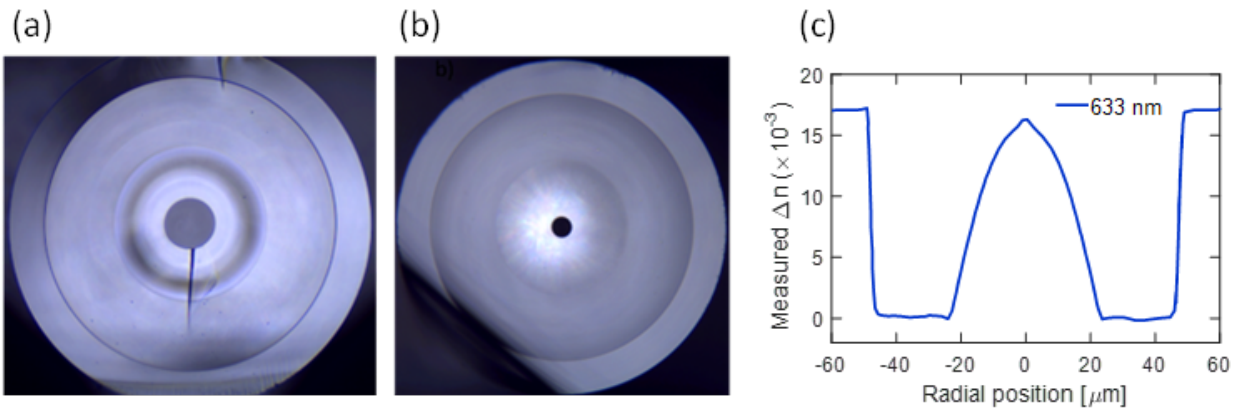
Figure 2.7: a) Cross section of the tube used for the fabrication of the graded index photonic lantern, consisting of a three-layer structure, the inner layer is the graded index region, the middle layer is a fluorine doped region to confine the modes at the lantern output after tapering, the outer layer is a silica layer. b) Partially collapsed tube for measuring the refractive index profile. c) Refractive index measurement of the tube used to fabricate the PL, we can clearly see the parabolic profile corresponding to the inner layer.

In this work we propose a novel method to fabricate a PL with a graded index core. It consist of having a capillary tube with three layers as shown in Fig. 2.7 (a), an outer layer of silica, a second layer of fluorine doped silica and a third layer of a fluorine doped silica with a graded index profile. To measure the refractive index profile of the different layers, a collapsed tube drawn to a fiber size was used as shown in Fig. 2.7 (b). Fig. 2.7 (c) shows the measured parabolic index profile of the tube used for the fabrication of a graded index core PL.
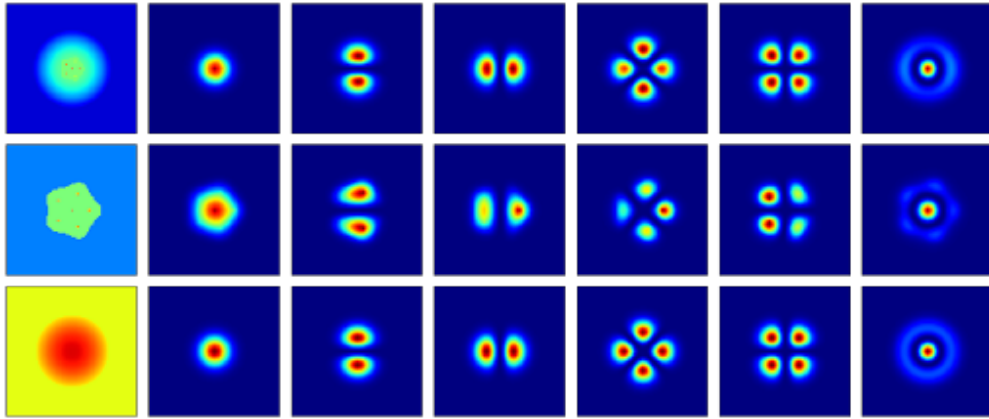
Figure 2.8: Calculated mode profiles of a) Graded index core photonic lantern b) step index core photonic lantern and c) six mode transmission fiber.

Fig. 2.8 shows the simulation results for the mode profiles for (a) the proposed graded index PL, (b) step index core PL where we see that the modes resemble those of the FMF, however, appear to be distorted into a pentagon shape, taken from the initial stacking of individual fibers into the fluorine-doped capillary, this leads to a slight mismatch when spliced to the transmission fiber. In (c) we see the calculated mode profiles of the GI-FMF. From Figs. 2.8 (a) and (c) we can see that the modes can be matched better when compared to the step index core PL case and we can expect a reduction on MDL and insertion loss to the transmission fiber.

17

Further analysis as shown in Fig. 2.9 shows the modal evolution as the lantern diameter is decreased along the taper. In an adiabatic taper, the launched modes follow each effective index line (propagation constants). If the lines do not cross then there is a one-to-one mapping between the output modes and input modes. At the point C the light is mainly confined in the individual cores with some coupling to adjacent cores, in B the modes are almost formed but are distorted and in A the whole set of modes match the GIF. The mode effective indices are plotted against the core diameter of the PL along the transition starting at 140 μm. At the input, we choose to have 4 different core sizes for the input fibers, i.e. 4 different propagation constants (4 separated blue curves at 120 μm), as the diameter decreases the cores begin to couple and then evolve into each specific mode of the final few mode PL output. At the PL output, there are only 3 groups of degenerate modes. The propagation constants are separated during the entire taper, ensuring that the output mode profiles corresponding to each propagation constant evolve into the modes of the PL output.
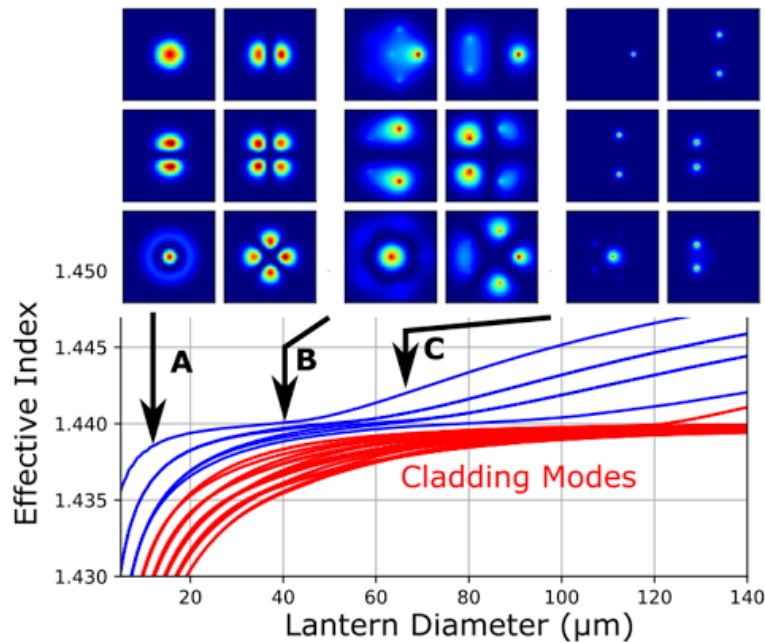
Figure 2.9: Mode evolution along the tapered transition of the photonic lantern as function of the effective index.

Fig. 2.9 (a) shows the simulation results for the case of having a step index PL, The MDL and modal crosstalk is simulated against the lantern core diameter. One can obtain a low MDL value when the core is around 17 μm, however, if we look at the modal crosstalk it is only below 2-dB, one can obtain better modal crosstalk performance if the PL is further tapered down but we also lose as the MDL increases for smaller lantern core diameters. Fig. **??** (b) also shows the simulated MDL and modal crosstalk as the lantern core diameter varies, this case is for the proposed graded index core PL, we observe that an MDL value of 0-dB is theoretically possible and also there is a bigger range for lower modal crosstalk compared to the step index PL case.
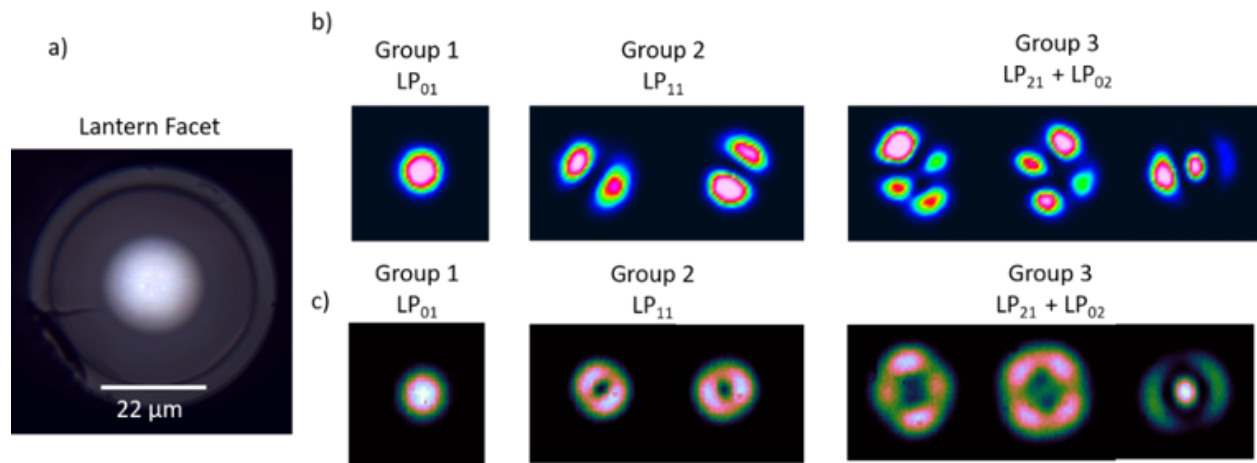
Figure 2.10: a) Microscope image of the fabricated graded index photonic lantern, b) Near field mode profiles at 1550nm at the lantern output, c) Near field mode profiles after FMF propagation over 5m.

The fabrication process for the graded index PL consists of dissimilar inserted into the capillary showed in Fig. 2.7 (a), to ensure mode selectivity on the device, the input fiber cores used are 1x23 μm, 2x18 μm, 2x15 μm and 1x11 μm for each LP01, LP11, LP21, and LP02 modes respectively with 125 μm cladding for the first three core sizes and 86 μm for the smallest core fiber. The capillary is tapered adiabatically by a factor of 44 using a CO2 laser tapering station with a total transition length of 8 cm, the obtained PL is 52 μm in diameter and has a core diameter of 22

µm. As we can see in Fig. 2.9 as the capillary is tapered down, the light cannot be confined in each individual core and starts coupling to the neighboring cores, subsequently the light is coupled to the graded index ring in the initial tube and is confined by the fluorine doped region. The contribution from the pentagon-shape initial stacking profile is negligible as the PL is tapered by a factor of 44, at the end the light will be distributed over the graded index region of the capillary.
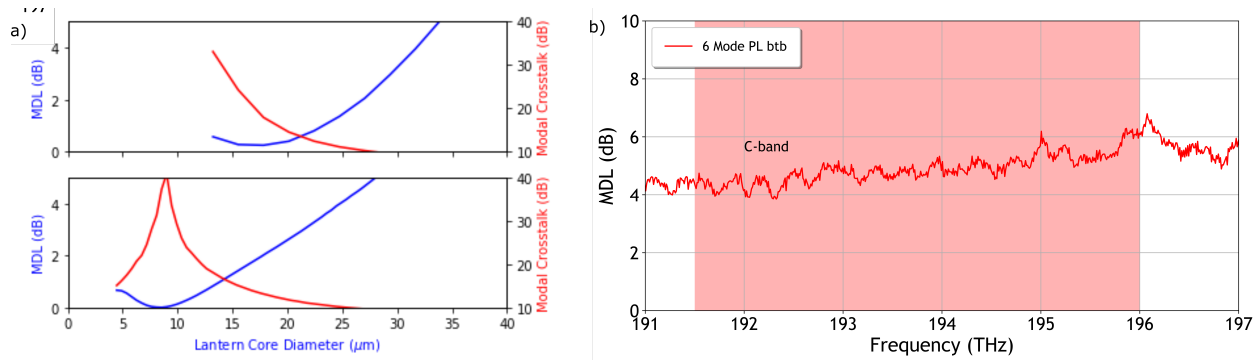
Figure 2.11: a) Plots of MDL and modal crosstalk calculation as function of the lantern core diameter for step index photonic lantern (upper plot), and graded index photonic lantern (lower plot). b) Measured MDL for the fabricated graded index photonic lantern

Characterization and results

Fig. 2.10 (a) shows the cross section of the fabricated device, the core of the lantern is formed by the cladding of the input fibers and the graded index region represented in the initial capillary, the light from the input fibers experience a smooth transition to the graded index region of the tube. Fig. 2.10 (b) shows the near field mode profiles at the output of the lantern facet at 1550 nm, using a super luminescent diode (SLD) as input source, we can clearly see nice and rounded mode shapes compare to those from a step index core lantern as showed in Fig. 2.2. After coupling into a graded index FMF supporting 6 spatial modes, the mode profiles are recorded as shown in Fig. 2.10 (c). The measured insertion losses at the lantern output are 0.1-dB for the LP01, 0.2-dB for the second

mode group and average 0.4-dB for the last mode group, which is comparable to the losses of step index PL [14].

After splicing to the GI-FMF, the insertion losses are between 0.5-dB for the LP01, 0.5-dB average for the second mode group and 1.9-dB average for the last mode group, this is due to mode size mismatch between the PL and the FMF cores as we are limited by the final size of the PL, going to a smaller core diameter to reduce IL and MDL will mean smaller cladding size of the PL which is already 52 μm in diameter, this will make it very difficult to handle for splicing to the transmission fiber.
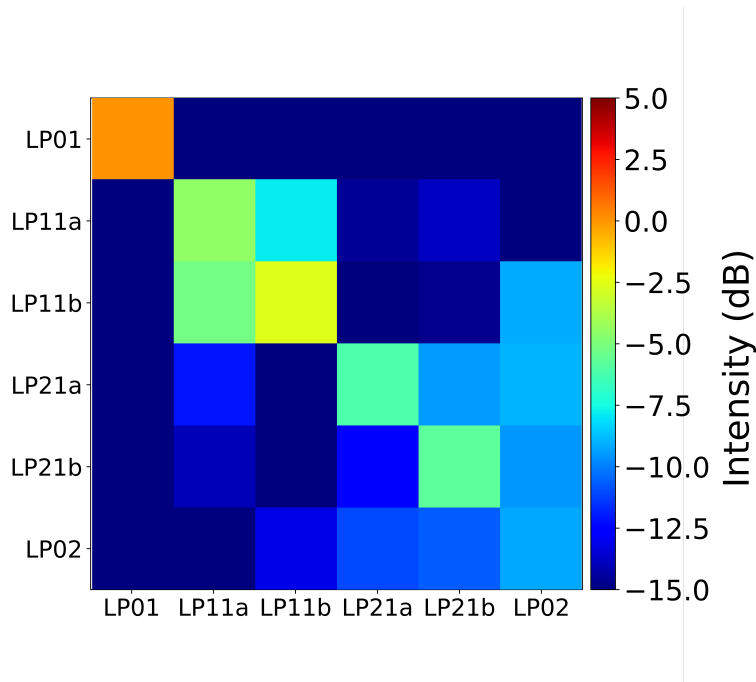
Figure 2.12: Measured TM of the graded index photonic lantern spliced to GI-FMF using a swept-wavelength interferometer in reflection mode.

Fig. 2.12 shows the measured TM for the fabricated graded index PL, spliced to a 5-meter long piece of GI-FMF, we see that the fundamental mode has no crosstalk to higher order modes, the second mode group sees more crosstalk and finally the third mode group has more crosstalk as the

lantern is not able to excite this mode group in the PL, this is also due to the mismatch in mode sizes as the PL has a rather large (20 μm)core compared to the required ideal core diameter (8 μm) to obtain the lowest MDL value as calculated from the simulations in Fig. 2.11 (a).We have demonstrated a mode selective PL with a graded index core, the modes at the output of the PL are a much better match to a graded index transmission FMF than those from a PL with step index core. Ultimately, the graded index shape will enable mode multiplexers without any insertion loss, that perfectly match the transmission fiber.

High spatial density photonic lantern for few-mode multicore fiber

To date, different types of fibres, such as single-mode multicore, few-mode, few-mode multicore and coupled-core fibres have been investigated to further increase data transmission. Specially, few-mode multicore fibres (FM-MCFs) have the advantage of drastically improving the fibre capacity combining multiple cores supporting as many modes as the fiber is designed to have, with the limitation of having to couple different modes into each of the different cores in the FM-MCF in a low loss and reliable way, here is where having a few mode multicore PL multiplexer can provide with the requirements needed for this specific fiber types, with the advantage of being an all-fiber device that can be directly spliced to the transmission fiber, reducing the footprint of the device.

Design and fabrication

The few-mode multicore PL mode multiplexer presented in this section comprises a series of concatenated individual tapered bundles. To ensure mode selectivity in the device, dissimilar fibres are used to remove the degeneracy between modes by having different initial propagation constants.

22

We use graded index fibres with an index contrast of 30×10^{-3} between core and cladding to relax the adiabatic requirements during the tapering process. Each of the initial tapered bundle is made by inserting six dissimilar graded index fibres with core diameters of 1 x 23.3 μm, 2 x 22 μm, 2 x 20.8 μm and 1 x 14.5 μm into a low refractive index capillary. The fibres are inserted into the capillary shown Fig. 2.13 (a) in which the index contrast with respect to silica is -15×10^{-3} following the core geometry presented in Fig. 2.13 (b). The capillary has an outer diameter of 490 μm and inner diameter of 345 μm, with a fluorine layer diameter of 420 μm and is initially tapered down using a CO2 laser glass processing machine to a size of around 260 μm, as presented Fig. 2.13 (c), at this point of the taper, the light is still confined into each individual core of the graded index fibres, thus, no coupling exists between cores.
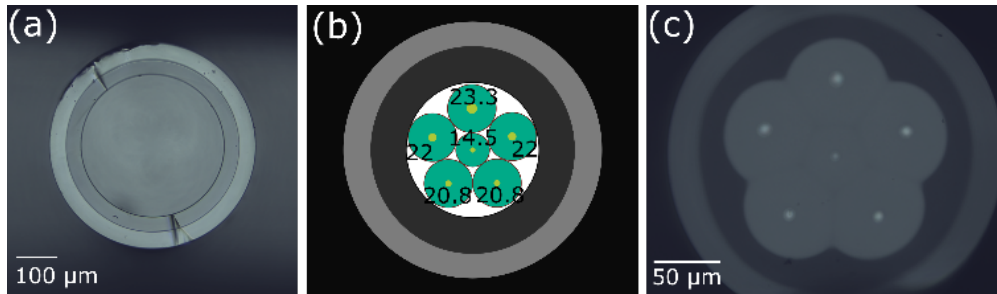
Figure 2.13: Fluorine-doped capillary used for the fabrication of each individual fibre bundle, (b) Geometric arrangement of the fibres used for each fibre bundle, (c) Microscope image of the fabricated fibre bundle after the first taper, before inserting into the capillary template.

In the next step, 7 of the fabricated tapered bundles are inserted into each hole of the microstructured glass template shown in Fig. 2.14 (a). The microstructured glass template is fabricated by the stack and draw method, made by inserting seven capillaries into a jacketing tube in a hexagonal array, the empty space in between those capillaries is filled with silica rods, notice that each of these capillaries has a low refractive index fluorine-doped layer with an index contrast of -9×10^{-3} with respect to silica. The preform is drawn to smaller canes with outer diameter of 1940 μm and hole diameter of 275 μm. The use of a microstructured template improves the core position

accuracy and can scale to a larger number of modes by increasing the inner diameter and the number of channels similar to the manufacturing process of multicore fibres, providing accuracy and repeatability.
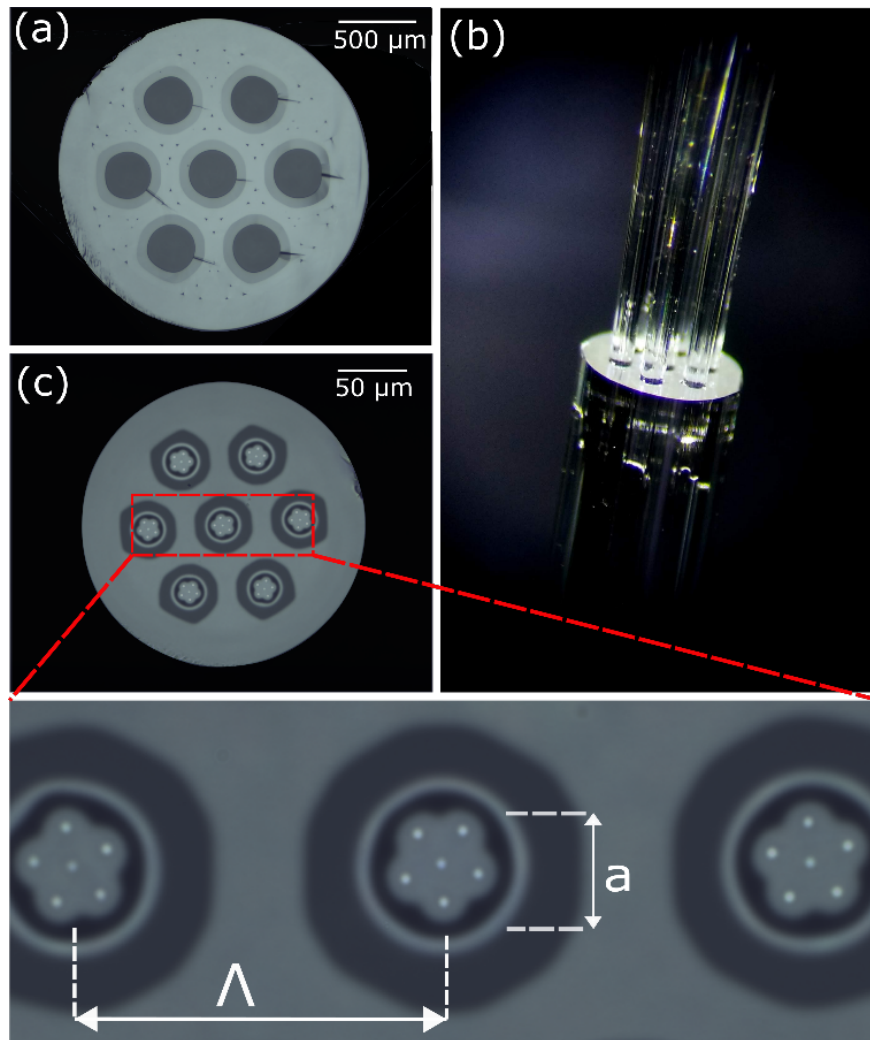
Figure 2.14: a) Cross sectional image of the microstructured glass template, b) Image of the glass template after inserting seven initially tapered bundles. c) Cross sectional image of the fabricated device after the microstructured template is adiabatically tapered, d) zoomed portion of the PL cores where represents the core to core distance and the parameter a represents the core diameter of the PL.

Figure 2.14 (a) presents the microstructured glass template used for the fabrication of the multi-

core PL, in Fig. 2.14 (b) 7 of the tapered fibre bundles shown in Fig. 2.13 (c) are inserted into the microstructured glass template and then a CO_2 laser glass processing machines is used to adiabatically taper the entire device first to a size of 800 μm with 25mm in the transition length to ensure adiabaticity. In the last step, the multicore PL is tapered down to a size of 210 μm over a length of 40mm. A cross section image of the fabricated multicore PL is presented in Fig. 2.14 (c). At the few-mode multicore end of the PL, the light in each individual core is confined within the fluorine doped layer. The initial fibres are the core of the PL and the low refractive index material surrounding it becomes the cladding of each individual PL core. The fabricated few-mode multicore PL has 7 cores with an average diameter of $\approx$ 18 μm, the fluorine layer that confines each core has a diameter of 23 μm and the separation between each core Λ is   54 μm (Fig. 2.14 (d)). At the multicore-few-mode end of the PL, 42 spatial channels are selectively excited.

Characterization and results

The few-mode multicore PL is characterized by exciting each of the individual input fibres, one at a time, with light from a super luminescent diode centred at 1550nm with 50nm bandwidth, the output near field images of each mode are recorded using a CCD camera and are shown in Fig. 2.15 for each PL core. The average loss across all of the seven LP01 modes is measured to be 0.2 dB, for the LP11a, b set of modes is 0.4 dB, for the LP21a, b set is 0.5 dB and across the seven LP02 modes is 2 dB. The high insertion loss in the highest order mode can be explained by the thin layer of fluorine-doped material that allows for the LP02 to leak out to the layer of silica in between the 2 fluorine-doped layers. This can be addressed by using an initial capillary with a thicker layer of low refractive index material or by removing the silica layer in between the fluorine-doped layers, this would create a double cladding protection for the PL core, expected to relax the adiabatic requirements of the taper.
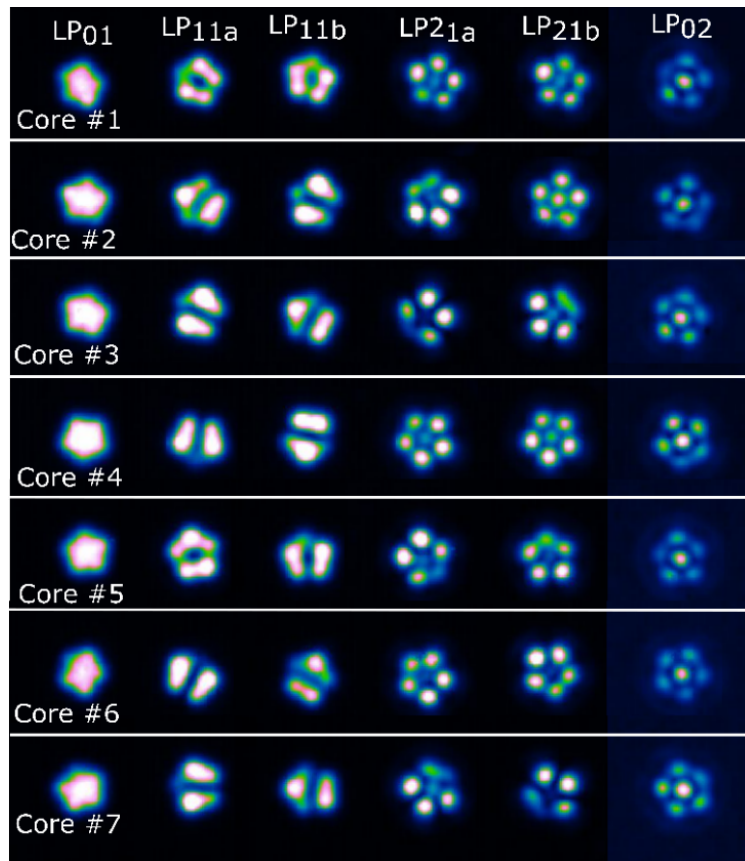
Figure 2.15: Near field mode profiles for individual cores in the multicore PL showing six spatial modes per core.

The fabricated device can be designed to match existing few-mode MCFs, to show the device preformance when splice to FMF, a 5-m long piece of FMF supporting six spatial modes is used to couple the central core of the fabricated device as shown in Fig. 2.16. Fig. 2.16 (a) represents the schematic of the coupling between the fabricated PL and the FMF supporting six spatial modes. Fig. 2.16 (b) shows the near field mode profiles after propagating through the FMF, notice that the device is able to selectively excite each of the modes in the FMF. The modes are excited using the same super luminescent diode centered at 1550nm. After splicing to the FMF, the measured IL for the LP01 is 0.7-dB, for the set of LP11 mode is 1.2-dB, in the case of the LP21 set, 1.5-dB is
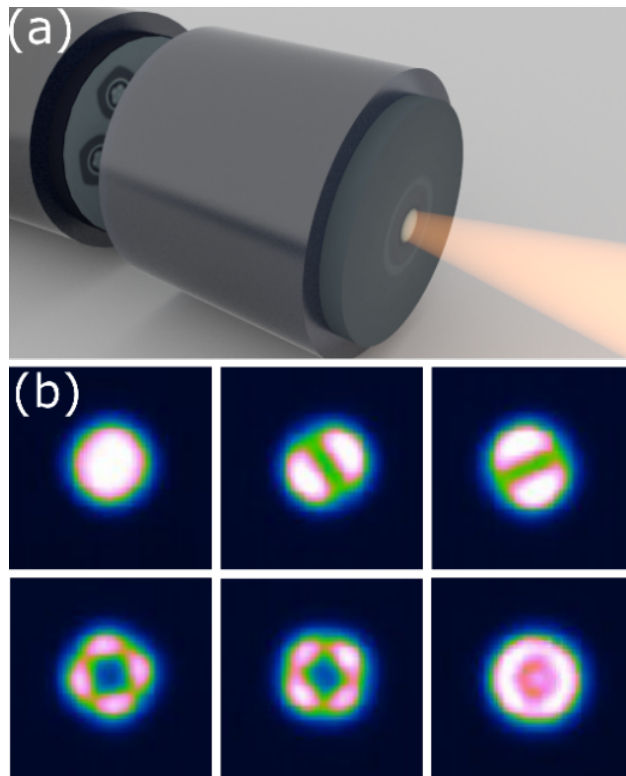
Figure 2.16: a) Schematic of coupling between the central core of the few-mode multicore PL and FMF, b) Near field mode profiles after transmission over 3 meters of FMF supporting six spatial modes.

measured, and 3.5-dB IL for the LP02 mode. The high insertion loss is due to the mode mismatch between PL and FMF, the LP02 mode has the highest IL due to the leakage into the cladding along the taper. Further optimization is needed to reduce the insertion losses to the FMF, this can be done by tailoring the index profiles of the glass template and the initial fiber size and index profile.

Conclusions

In this chapter I have demonstrated different types of PL mode multiplexers for different types of few mode transmission fibers, in the case of step index FMF, a device with record low MDL for

S+C+L communication bands has been fabricated, with the lowest being in the C-band with only 0.8 dB MDL, 1 dB for the L-band and up to 1.5 dB for the S-band per mode multiplexer. In the case of GI-FMF I have demonstrated a graded index photonic lantern concept which can be integrated into GI-FMF links, this device reduces the MDL due to the better overlap between the modes in the PL and the GI-FMF and can potentially enable mode multiplexer with very low insertion loss by perfectly matching the transmission fiber. In the last section I have demonstrated the feasibility of increasing the mode density of the PL to 42 spatial modes in a single device, which is the highest number of modes reported for a PL mode multiplexer, this concept enables the transmission over few mode multicore fibers and can be extended to fibers with multiple number of cores/modes. As shown in this chapter PL mode multiplexers are very versatile devices that can be designed for a wide range of FMFs with step or graded index profiles and which scalability is also possible by using microstructured glass templates.

CHAPTER 3: FIBER BUNDLE FAN-IN/FAN-OUTS FOR MULTICORE FIBERS

Introduction

SDM has been extensively investigated as a promising solution to increase the capacity of data transmission above the SMFs limit. One of the approaches consists in the use of uncoupled MCFs [27, 28, 29, 3, 9, 30]. MCFs offer the possibility to have different single-mode channels sharing a single cladding, thus increasing the amount of transmitted data by the number of cores present in the MCF, resulting in a practical single-fiber solution. MCFs with homogeneous cores can achieve higher transmission capacity without requiring advanced multiple input-multiple output (MIMO) receivers.

One of the challenges for uncoupled multicore fibers is the fabrication of fan-in/fan-out (FIFO) devices with low insertion loss and high core count that are required to couple to each individual core of the MCF. FIFO devices are not only needed for multicore fibers, they can also be used for coupled-core fibers [31, 32] and coupled-core amplifiers [33]. Over the past few years, several types of FIFO devices with different number of cores have been proposed for single mode MCFs including fiber bundles[34, 35, 36], 3D waveguides[37, 38] and free space optics[39].

19-core fan-in/fan-out device based on reduced cladding graded index fibers

In this section I present the fabrication of a 19-core FIFO device for an uncoupled single mode 19-core fiber using a micro-structured template and reduced-cladding graded index fiber as mode field adapters for the single mode cores in the MCF and regular SMFs as inputs/outputs. The device

consists of 19 individual graded index fibers with 35 μm and 85 μm core and cladding diameter, respectively.

One important characteristic to reduce the splice loss is to match the mode field diameter (MFD) in both fibers to splice, additionally, in the case of MCFs the rotational alignment also plays an important role, as core misalignment can introduce additional coupling loss or polarization dependent loss (PDL) as offset alignment can occur. In MCFs in order to acces each core in the fiber one has to match the number of cores to SMFs at the input/output of the MCF, this can be realized by using a bridging device that provides low splice loss at the SMF side and also at the MCF side.
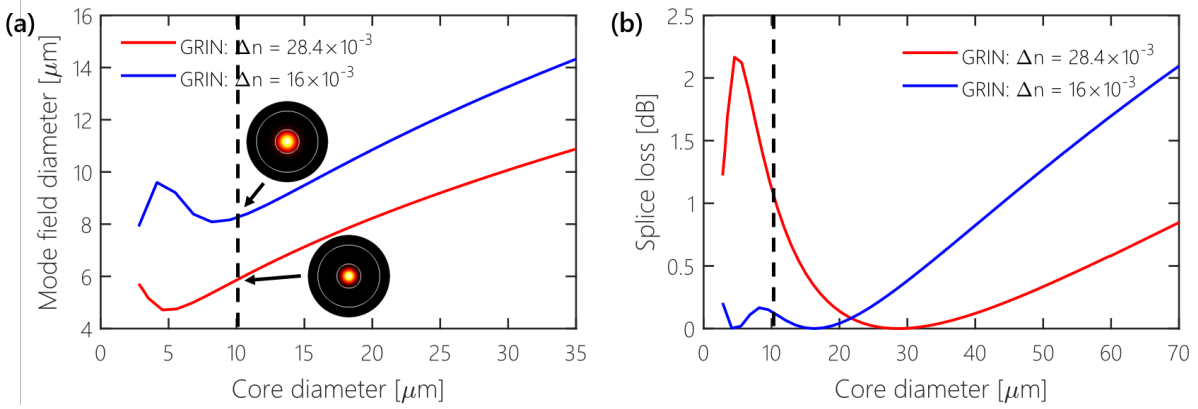
Figure 3.1:   Plots of a) Mode field diameter evolution for two graded index fibers with different index contrast of 28.4x10 $^{-3}$ and 16x10^{-3}, b) Calculated splice loss to the MCF fiber.

In this section I present the use of a microstructured glass template made out of pure silica in addition to reduced-cladding graded index fiber for FIFO fabrication. The glass template is realized by the stack and draw method to provide the input channels in which the graded index fibers are inserted. Graded index fiber with a specific index contrast are used so that the mode field diameter before and after the taper matches that of a SMF and the MCF. This fiber is designed to keep the mode field diameter as close as possible to that of the MCF after tapering. Reduced-cladding fiber allows to decrease the taper ratio, increasing the adiabaticity requirements as less material is added

before tapering, preventing the MFD in the fiber to change abruptly along the taper, in this way one can achieve low loss splices at the SMF and MCF sides.

Design and fabrication

The FIFO device was fabricated with the goal to reduce the coupling loss to a trench-assisted MCF with a core-to-core distance of $35\mu m$ and a mode field diameter of 9.84 μm at 1550nm. We fabricated two fibers with the same core and cladding diameter but with different index contrast of $16x10^{-3}$ and $28.4x10^{-3}$, respectively. Figure 3.1a shows the mode field diameter (MFD) plotted as function of the core diameter for both fabricated fibers. From Fig. 3.1a we can observe that the MFD for the lower index contrast fiber decreases to about 8 μm when the core diameter is around 10 μm, whereas in the case of the fiber with higher index contrast, the MFD is decreased to about 6 μm when the core size is around 10 μm. Figure 3.1b shows the splice loss to the MCF as a function of the grade index fiber core diameter. It is important to notice that at the end of the tapered section, each graded index fiber core diameter is approximately $10\mu m$. The splice loss to the MCF is reduced for the case with the fiber with the lower index contrast, thus, for the fabrication of the actual device, graded index fiber with lower index contrast are preferable as they can provide low splice loss at both MCF and SMF ends.

To fabricate the fan-in/fan-out device, 19 core individual fibers with a 35 μm and 85 μm core and cladding diameter, respectively, are inserted into the capillary shown in Fig. 3.2b. The capillary was fabricated using the stack and draw technique, and the diameter of the capillary is only 730 μm while each hole has a diameter of 90 μm. Using a CO_2-laser glass processing machine, the fiber bundled is down tapered by continuously heating and elongating the capillary. The taper ratio is set to about 3.4 in order to match the pitch of the MCF as shown in Fig. 3.2a. Fig. 3.2c shows the cross section of the fabricated fan-in device showing the individual cores after tapering the
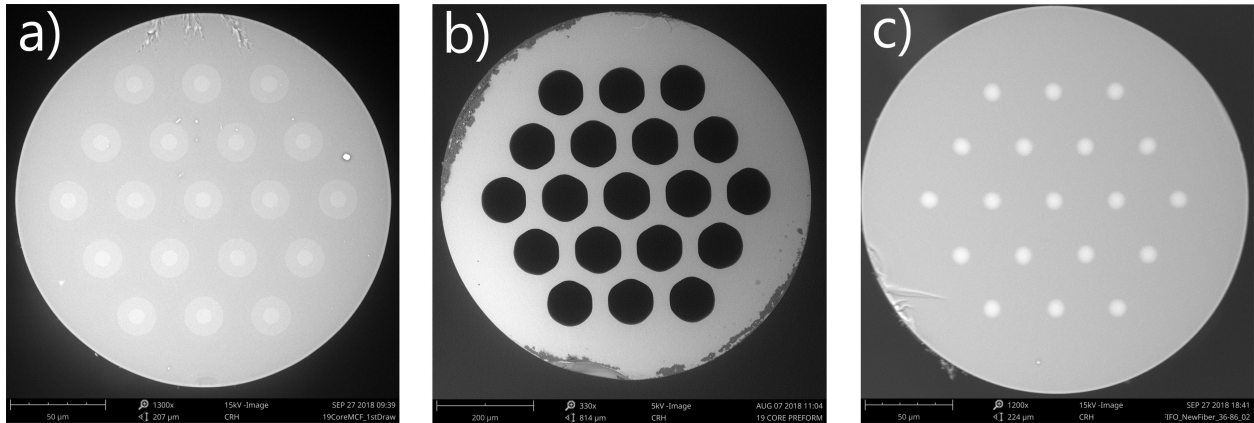
Figure 3.2: SEM cross-section pictures of a) fabricated MCF, b) micro-structured preform used for the FIFO fabrication, and c) fabricated FIFO device.

capillary. Each core measures around 10 μm after tapering, and the theoretical MFD at this point is calculated to be 8.3 μm with a theoretical splice loss is only 0.2 dB to the MCF. The hexagonal array at the end of the taper matches precisely the core arrangement of the multicore fiber with only a small variation in the pitch of less than 0.5 μm. After the taper, the fundamental mode is still confined in each individual core, and low crosstalk is observed with the neighboring channels.
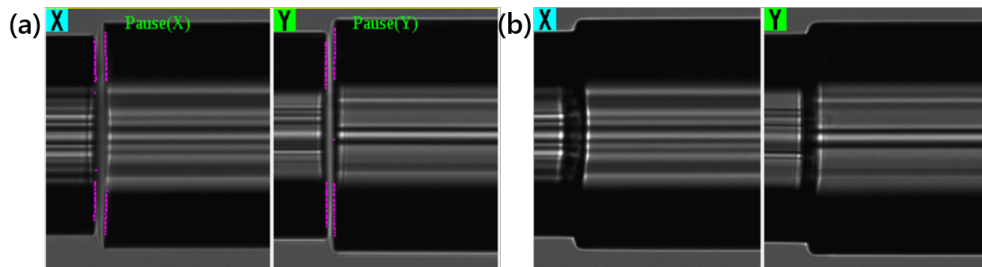
Figure 3.3: a) cladding alignment of both fiber and FIFO, b) x and y view after the splice

Fig. 3.3 shows the alignment and splice of the MCF and fan-in device using a CO_2-laser splicer unit, one of the most important points when making the devices is to have the core to core distance to be the same as that of the MCF, but is also very important the rotational alignment of the cores

to have a good overlap between the cores, core misalignment due to rotational alignment and core pitch leads to increase on the splice loss. Another important parameter is the cleave angle in both, fiber and FIFO, the case shown in Fig. 3.3a shows cleave angles of 0.3 a 0.1 deg for fiber and fan-in/fan-out respectively, having low cleave angles gives better performance during the splice as the end-facets are almost flat. The arc power used is lower compared to that required for a SMF splice but enough to joint them together, when using higher arc power the splice will look like a taper due to the difference in cladding diameters and it will cause to the cores in the outer ring to have a higher splice loss. In Fig. 3.3b, after the splice we still see the boundary of the fiber and FIFO showing that the cores in the outer ring will not have a high splice loss as no significant distortion is seen.
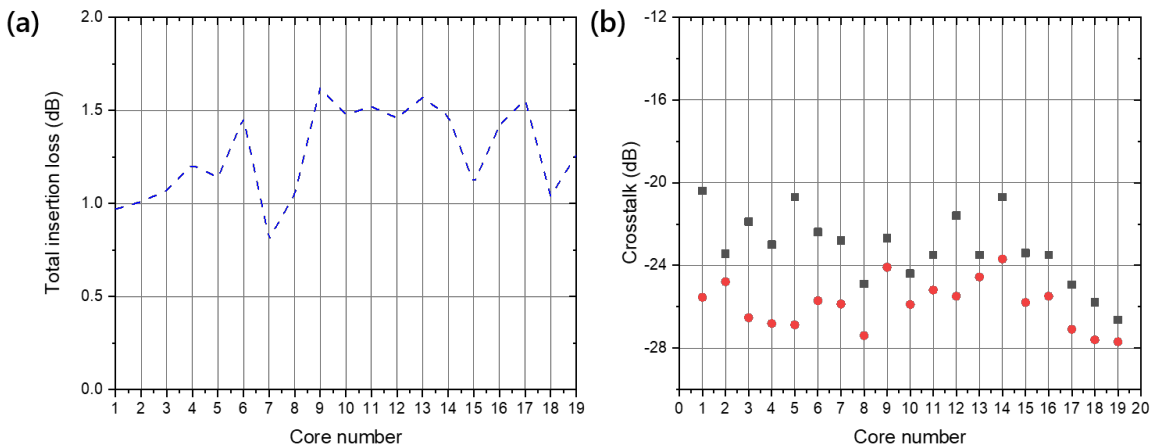
Figure 3.4: a) Total insertion loss for a pair of FIFO devices spliced to 3 m of trench-assisted 19-core fiber. b) Measured crosstalk, black squares indicate the highest crosstalk value and the red dots indicate the lowest crosstalk value measured.

Characterization

After splicing two FIFO devices to 3m of the trench-assisted MCF, insertion loss was measured using a laser source centered at 1550 nm, exciting individual cores with a SMF and measuring the output power at the corresponding core using an optical power meter. The obtained average insertion loss for two FIFO devices is only 1.27-dB with insertion loss variation of 0.8-dB as shown in Fig. 3.4(a), the lowest insertion loss obtained was 0.81-dB and the biggest one of 1.62-dB for a pair of devices. To measure crosstalk, each individual core was excited and the power in the closest neighbors was measured. Fig. 3.4(b) shows the measured crosstalk, the blue triangles represent the highest crosstalk values and the red diamonds represent the lowest crosstalk value, in general an average crosstalk of <-20-dB is measured.

4-core and 7-core fan-in/fan-out devices for multicore fiber

This section presents the fabrication of fan-in/fan-outs for MCFs supporting 4 and 7-cores. These fibers are one of the simplest MCFs and have similar characteristics to SMFs while being able to hold multiple SMFs within the same standard cladding diameter. One of the most simple and common MCF type is that one having 4-cores within a 125 μm, this fiber offers 4 times the data capacity transmission compare to SMF, having almost the same loss and characteristics of the SMF counterpart. This fiber is believe to be a potential candidate for future submarine and terrestrial networks. One of the main challenges is coupling light into each of the cores individually with high efficiency and low crosstalk. In this section I present the results on the fabrication and characterization of a FIFO device for a 4-core MCF and further extend its applicability when implemented into a 7-core MCF.

The fabricated devices are designed to reduce the insertion loss to MCFs with 4 and 7 cores, the MCFs were fabricated by ourselves. These fibers are designed to have similar characteristics compare to SMFs. Coupling light into these fibers implies matching the SMF part on one side to the MCF on the other end. The 4-core and 7-core FIFO devices were fabricated to have low splice loss at both SMF and MCF ends. A fiber bundle approach is used for the fabrication of both 4-core and 7-core FIFO devices where a bundle of fibers (4 or 7) are used as initial fibers and then tapered to match the core to core distance in the MCF similar to the case for 19-core FIFO. These fibers are designed to have low splice loss to the SMF end.

Core number	1	2	3	4
1	**-0.41**	-61.2	-63.6	-63.4
2	-61.8	**-0.32**	-62.8	-62.7
3	-63.8	-63.1	**-0.35**	-63.2
4	-63.4	-62.7	-61.5	**-0.32**

Table 3.1: Measured insertion loss (dB) and crosstalk (dB) at 1550 nm for a pair of FIFOs spliced to 10-m of MCF.

Table 3.1 summarizes the measured insertion loss and crosstalk for a pair of FIFOs spliced to a 10-m long piece of MCF. Light from a laser source at 1550 nm is used to characterize the MCF link, light is coupled to one of the FIFO cores and measured at the output of the second FIFO with an optical power meter. The lowest insertion loss is 0.32-dB which is the lowest loss reported to a 4-core MCF, the highest measured loss is 0.41-dB and this difference can be explained due to core misalignment during the splice or losses over the taper. The measured crosstalk to the other channels is < -61.2-dB which shows that this FIFO can be exploited for MCFs in submarine or

terrestrial networks due to the relatively high coupling efficiency and low crosstalk. The performance of these FIFO devices is key for MCF to be used in long distance transmission scenarios. It is important to notice that the losses presented here are for a pair of FIFO and the loss for each individual core in the FIFO is on the order of 0.2-dB or less. The results presented in this dissertation show that record-low loss FIFO devices can be design and fabricated and this can allow for potential commercialization of MCF for submarine of terrestrial networks.

Core number	1	2	3	4	5	6	7
1	**-2.32**	-56.3	-51.6	-51.4	-46.4	-49.1	-48.1
2	-56.3	**-2.04**	-48.3	-61.3	-61.3	-63.2	-51.7
3	-46.5	-47.6	**-2.14**	-57.8	-62.4	-60.3	-61.3
4	-50.4	-59.4	-56.7	**-1.87**	-48.1	-59.5	-58.8
5	-45.9	-59.3	-61.1	-49.1	**-2.11**	-59.6	-61.6
6	-48.5	-55.4	-60.2	-58.8	-57.2	**-2.19**	-51.5
7	-54.3	-48.6	-62.2	-63.7	-61.6	-50.9	**-2.17**

Table 3.2: Measured insertion loss (dB) and crosstalk (dB) at 1550 nm for a pair of FIFOs spliced to 5-m of MCF.

Table 3.2 shows the characterization results of the fabricated 7-core MCF after splicing to the a 5-m long piece of 7-core MCF, note that the measured loss includes that of the SMF ends, the insertion loss varies from -1.87- to 2.32-dB for a pair of 7-core FIFO devices with crosstalk values below -45.9-dB. Further coupling efficiency can be achieved by tailoring the refractive index of the initial fibers to match SMF and MCF.

Conclusions

On this chapter I have presented the fabrication of different FIFO devices for 4, 7 and 19-core MCFs. Different approaches have been proposed and studied in order to increase the coupling efficiency to MCFs. A 4-core FIFO was fabricated obtaining the lowest reported insertion loss to 4-core MCF of only 0.32-dB per core for a pair of FIFO devices, with crosstalk values below -61.2-dB. In the case of 7-core MCF, a FIFO was demonstrated with insertion loss ranging from 1.87- to 2.32-dB per core for a pair of FIFO devices and crosstalk values below -45.9-dB. High coupling efficiency FIFO devices can pave the way for MCF commercialization in terrestrial and submarine networks to replace the widely used SMFs.

Another approach has also been investigated where I have shown the design and fabrication of a 19 core FIFO device for a 19 core tench-assisted MCF with average insertion loss of 1.27-dB for a pair of devices and crosstalk $<$-20 dB with the neighboring channels. The use of reduced-cladding graded index fibers allows to better match the MFD at the tapered side of the device as the MFD does not change much for small taper ratios, this technique can be applied to higher core count MCFs and can be improved by designing the graded index fiber with an specific index contrast to better match the MCF.

CHAPTER 4: FEW MODE AMPLIFIER BASED ON COUPLED-CORE ERBIUM-DOPED FIBER

Introduction

In recent years, several MCF and MMF have been fabricated with the purpose of increasing the capacity in optical fiber communication links[27, 28, 29, 3, 9, 30, 40, 41, 8]. Coupled-core fibers (CCFs) look particularly promising as they have been shown to outperform equivalent single-mode fibers in transmission systems over long distances[42, 43] and they can be fabricated to have very-low loss[44].

SDM can upscale the capacity per fiber proportional to the number of modes in a few mode fiber. However, realizing such operation in long haul transmission systems requires the development of amplifiers and components that are compatible with FMFs. So far, transmission over FMFs has been shown for up to 45 modes [45]. The main limitations for SDM transmission over FMFs are differential mode group delay (DMGD) and mode dependent loss (MDL). Another promising approach to overcome the capacity limitation imposed by single mode fiber systems is the use of coupled-core transmission fibers. In these fibers, the strong random mixing between cores can reduce the buildup of nonlinear interactions [46]. Moreover, linear impairments are also reduced as the mode mixing ensures that every input signal propagates nearly equally on all cores which homogenizes any loss or delay differences between cores.

From an amplifier perspective, coupled-core fibers are attractive as they can be designed to provide low mode dependent gain (MDG) levels, as well as strong random mixing between all supported modes. As such, quite recently, coupled-core fiber amplifiers have been considered in a number of studies, demonstrating their potential for SDM applications [33, 47, 48, 49]. On the other hand, all

38
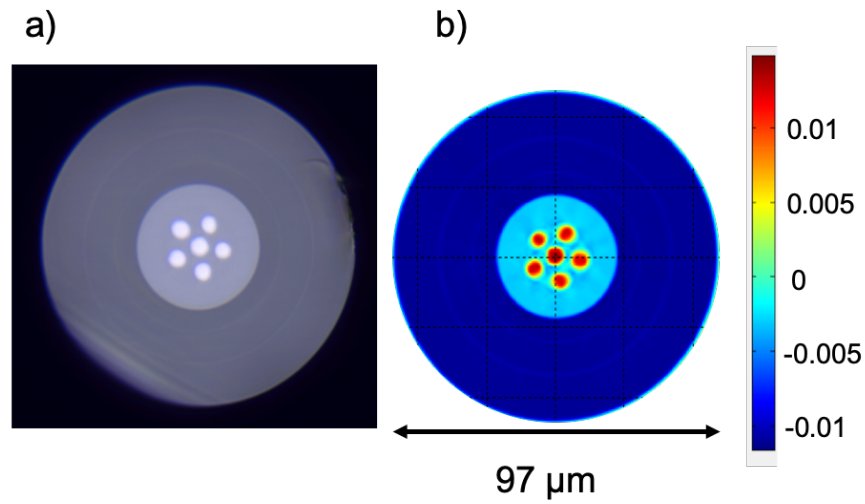
Figure 4.1: (a) Cross-section image of the fabricated 6-core coupled-core EDF. (b) Measured refractive index profile.

coupled-core amplifiers investigated to date are unsuited for FMF links [50]. Different approaches of coupled-core amplifiers have been demonstrated with up to 12 cores, showing high amplification efficiency and low mode dependent gain (MDG)[47]. One can think of the advantages of coupled-core regime such strong mixing to reduce MDL and incorporate it to few mode fiber links as another approach for amplification. The question naturally arises as to whether one can implement a coupled-core amplifier which can be integrated into a FMF transmission system. Here, I report for the first time a coupled-core amplifying fiber concept compatible with FMFs. The proposed 6 coupled-core EDF can be coupled with low-loss to a 6-mode FMF by a slight adiabatic taper, thus, allowing efficient mode conversion from a couple-core to FMF scheme.

Coupled-core amplifying fiber design and fabrication

The coupled core amplifier was designed to minimize both, MDL and differential group delay (DGD) when spliced to a 6-mode transmission fiber. A condition to achieve mode mixing in a multicore fiber has been reported in [33]. The coupled-core approach corresponds to a regime in which a set of cores, placed at appropriated distance between each other, in a multicore fiber behave like a single-multimode core with slightly different propagation constants thus allowing mode mixing when the fiber is subjected to perturbations. The coupled-core EDF was fabricated by inserting six erbium-doped rods into a silica preform with 6 drilled channels. Subsequently, the preform was placed inside a fluorine doped tube (Δn of -8.2×10^{-3}). A fiber was then drawn to an outer diameter of 97 μm and a low index polymer coating (NA ≈ 0.46) was applied in order to guide multimode pump light. The outer diameter has a strong impact on the amplifier properties and was designed to provide strong overlap between the pump and the active cores.
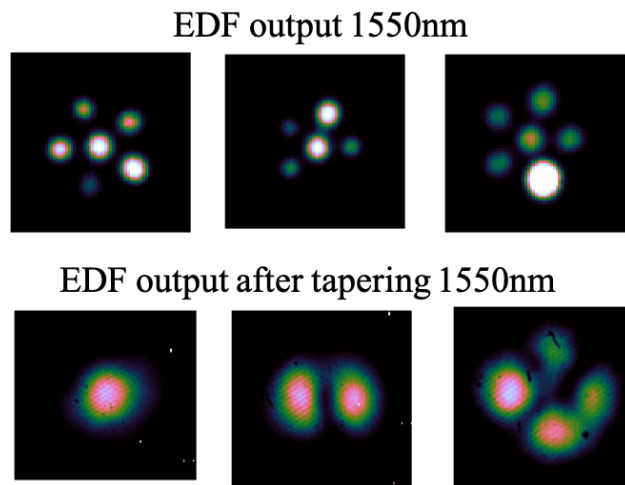
Figure 4.2: Near field mode profiles of the fabricated coupled-core erbium-doped fiber, before and after tapering at 1550 nm

Figure 4.1 (a), shows the cross-section microscope image of the 6 coupled-core EDF. The diameter

40

of inner silica region surrounding the Er-doped cores is 35 μm. The diameter of the Er-doped cores is approximately 5 μm and the core-to-core distance among the external cores is 7 μm. The distance between the central core and the external cores is 8 μm. The Er-doping concentration of the fabricated fiber is 4.5×10^{25} ions/ m^{-3}, the refractive index contrast of the Er-doped cores with respect to silica is $\Delta n \approx 16 \times 10^{-3}$. The measured 2D refractive index profile of the fabricated fiber is presented in Fig. 4.1 (b), clearly highlighting the F-doped, un-doped silica and Er-doped regions.
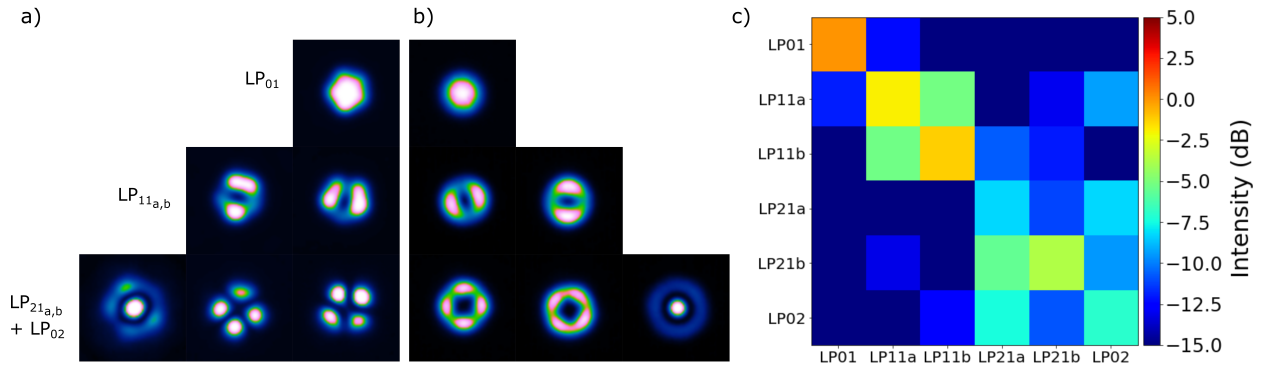
Figure 4.3: Near field mode profiles at the output of (a) photonic lantern and (b) after few mode fiber at 1550 nm. c) Measured transfer matrix for a pair of PL.

Amplifier assembly and characterization

In order to study the coupled-core to few mode compatibility of the 6-core EDF the near field intensity profiles of the fabricated coupled-core EDF were investigated in the near field at 1550 nm, Fig. 4.2 (top). As expected, the mode profiles are representative of a coupled-core fiber structure. In contrast, if the output end of the 6-core EDF is adiabatically tapered by a small ratio (≈ 1.3 times), the modes of the coupled-core fiber evolve into spatial modes of a FMF, see Fig. 4.2 (bottom). In this case, at the taper waist, the F-doped silica region of the EDF becomes the cladding of a new FMF, while the inner silica region becomes its core. The measured intensity profiles clearly

indicate that our tapered coupled-core EDF can efficiently generate FMF-like modes. Further, by tapering the EDF on both ends and splicing it to an input and output FMF, one can convert from FMF modes to coupled-core fiber modes and back to FMF modes in a low-loss fashion under the right tapering conditions. In other words, the tapered coupled-core EDF acts as a low-loss mode converter from FMF modes to coupled-core fiber modes and vice versa. Thus, allowing to implement a coupled-core amplifier in a FMF transmission link.

In this experiment mode selective PLs are used to characterize the performance of the amplifier design. A PL comprises a set of individual fiber inserted into a low refractive index capillary, then tapered adiabatically down to a multimode waveguide, where the initial fibers become the core and the low refractive index capillary becomes the cladding. By choosing dissimilar fibers as inputs, one can assure that the modes evolve into the modes of a few mode fiber. Moreover, PLs can be fabricated with low loss and be spliced directly to the FMFs as it is an all-fiber device which reduces the need of free space coupling. The PLs used in this experiment are spliced to 5m of graded index FMF supporting 6 spatial modes (LP01, LP11a, LP11b, LP21a, LP21b, LP02), the near field mode profiles at the output of a 6-mode PL and after splicing to the FMF are shown in Fig. 2.2 (a) and (b) respectively. Fig 2.2 (c) shows the transfer matrix from a the pair of PLs used in this experiment, we can see that good mode selectivity in the first two mode groups, the last group comprises the higher order modes supported by the FMF and some crosstalk is observed to the second mode group.

Having considered the linear properties of the coupled-core EDF, it is now important to assess the amplifier performance. Fig 4.4 depicts the experimental setup used to characterize the amplifier. We used two 6-mode selective photonic lanterns as mode multiplexer/de-multiplexer.Additionally, the measured MDL for the PL multiplexer pair is ≈2.5 dB across the C-band. A 3.5 m long coupled-core EDF was tapered on both ends, and spliced to the input and output FMFs, as illustrated in Fig. 4.4. The coupled-core EDF presents strong mode coupling at both signal and pump
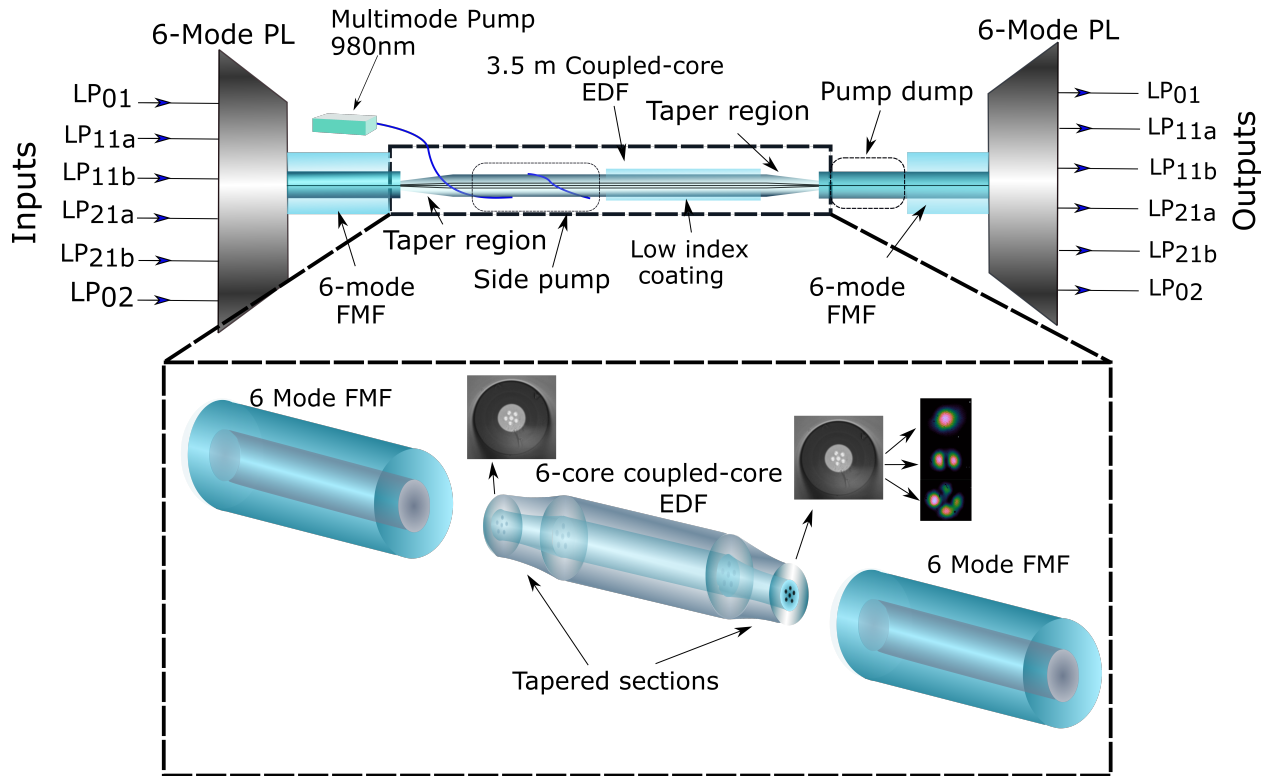
Figure 4.4: Amplifier characterization setup using two PLs to launch signal and side pump configuration.

wavelengths, indicating that the fiber could potentially be used in a core or cladding pumped configuration. However, in our experiments, the amplifier was cladding pumped. Pump light was side coupled into the EDF using a tapered coreless fiber spliced to a multimode pump diode. The coreless fiber was tapered down to 20 μm and wrapped 1.5 turns around the EDF. Pump light was then guided by the low index coating of the coupled-core EDF, see Fig. 4.4.
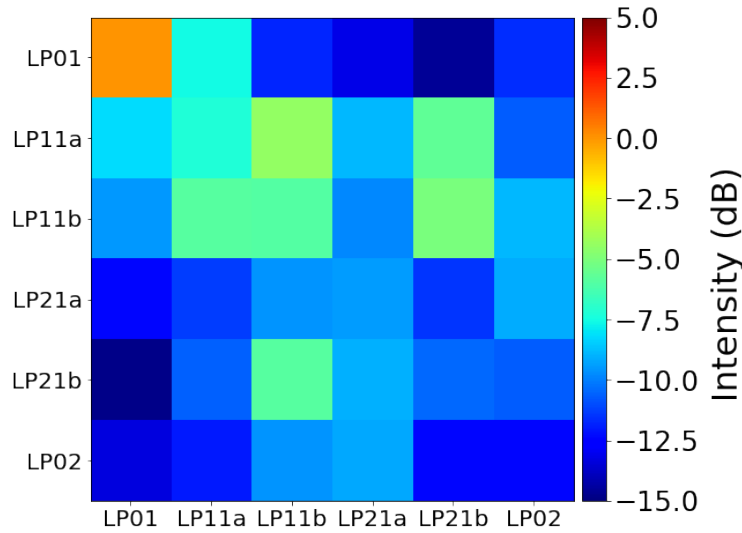
Figure 4.5: Transfer matrix when the coupled-core erbium-doped fiber is spliced between the 2 PLs.

Gain measurements from the transfer matrix

In coupled-core systems, core to core characterization is erroneous because each input evenly excites all outputs. The most accurate way to characterize the amplifier mode dependent gain (MDG) is to characterize the amplitude and phase transfer matrices (TMs) of the amplifier between each input and output pair across all wavelengths. The TM measures all possible paths through the multimode system. From the TM, we can obtain information about the MDL and mode average insertion loss (IL). Fig4.5 shows the TM of the amplifier, as we can see the TM is coupled and only some higher contribution of the fundamental mode is observed but the higher order modes are fully coupled, in this case we cannot characterize the amplifier by launching and receiving in each input and output. We used a swept-wavelength interferometer with spatial diversity [51] to measure the TM of the system. The EDF does not maintain mode selectivity as modes experience random scrambling in the coupled-core waveguide. An important feature of the coupled-core erbium-doped fiber is that it provides mode mixing which can reduce differential mode group

44

delay (DMGD) effects in FMF transmission links. By further optimizing the EDF, larger levels of mode mixing can be achieved.
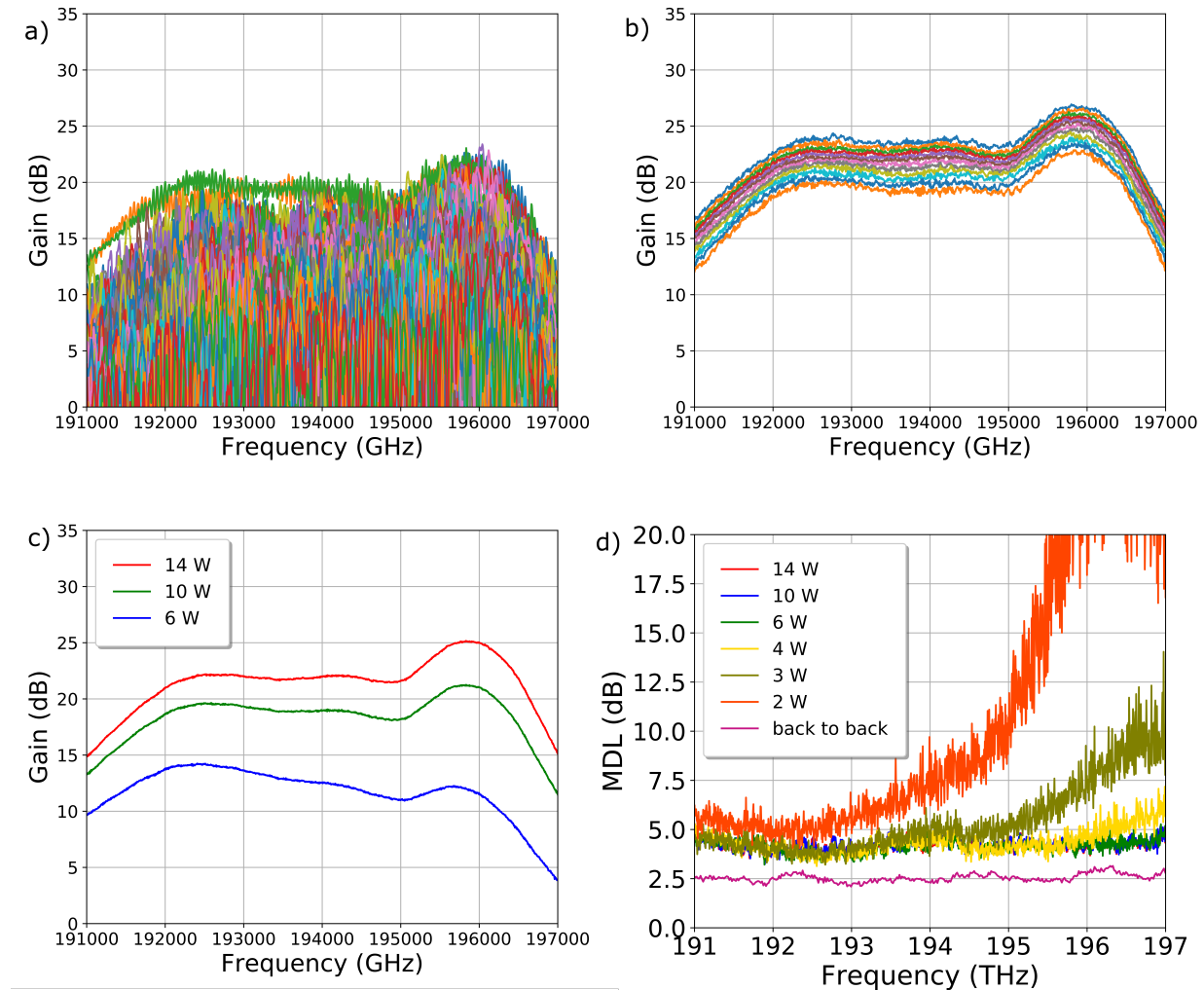
Figure 4.6: Gain measurements for a 3.5 m long EDF where (a) shows the 12×12 TM elements overlapped into one single plot b) 12 singular values (2 polarizations $\times$ 6 spatial channels) computed at each frequency c) MDL measured for a pair of lanterns back to back and for different pump powers in the amplifier.

Fig 4.6 (a)-(c) shows the gain measurements of the amplifier configuration and how the MDL and gain are extracted from the TM. Fig. 4.6 (a) shows all 12×12 TM elements overlapped into a

45

single plot. Due to strong modal mixing, which causes spectral fluctuations, it is impossible to accurately estimate the gain or MDL from core to core measurements. Fig. 4.6 (b) shows the 12 singular values (2 polarizations × 6 spatial channels) computed at each frequency which are used to obtain the mode average gain and MDL shown in Fig. 4.6 (c) and (d). From Fig. 4.6 (b) the largest singular value represents the the absolute maximum gain and the smallest singular value represents the absolute minimum gain, thus, the average of the singular values represents the average gain of the amplifier. In these highly coupled systems, MDL is the most important metric. A MDL of 0 dB means that all spatial and polarization modes have exactly the same gain through the system. In this case, an MDL ranging from 3.4-dB to 5-dB dB was achieved as seen in Fig 4.6 (d), it is also important to notice that these values of MDL include the 2.5-dB MDL measured back to back, thus, only 0.9-dB to 2.5-dB MDL is added to the amplifier by the coupled-core EDF. We can also observe the evolution of the MDL as the amplifier is pumped, for pump values over 4 W the MDL does not change under constant pump illumination up to 14 W of pump power.

Conclusions

This chapter discussed a novel concept of a coupled-core amplifier fiber concept compatible with FMFs, based on a coupled-core EDF.The 6-core coupled-core EDF can be spliced with low insertion and low mode dependent loss to a FMF supporting 6 modes via a slight taper transition. Strong mode coupling in the EDF reduces MDG and at the same time can provide mode mixing in FMF links. The fabricated amplifier concept provides over 20-dB gain over the C-band while adding only 1 to 2.5 -dB MDL to the FMF link. This amplifier concept can be scaled to FMF amplifiers supporting more modes.

CHAPTER 5: ASSEMBLY AND CHARACTERIZATION OF MULTIMODE ERBIUM-DOPED FIBER AMPLIFIER USING DIGITAL HOLOGRAPHY

Introduction

Different approaches of SDM have been investigated in recent years, one of the promising candidates is the use of FMFs or MMFs where different modes are used as transmission channels. In mode division multiplexing (MDM) systems, passive and active components are required, including mode multiplexers and multimode amplifiers able to compensate for the intrinsic loss of the fiber link over long distances. The challenge with building a multimode amplifier is achieving equal gain across the fiber modes. In other words, all modes need to have the same gain to equally amplify each channel. Additionally, there are several critical parts to a multimode amplifier including the input and output splices through which the transmission fiber modes are amplified, and each part contributes to the overall MDL and mode scrambling. Characterizing accurately the contribution to MDL and modal crosstalk of each step during the assembly of an amplifier is very important to reduce these impairments and obtain feedback at each point.

In the case of an ideal amplifier there is no mode mixing, each input mode couples to exactly the same output mode. Characterizing such an amplifier with N modes would require exactly N measurements. However, in the presence of mode mixing, each input mode can couple to every single output mode and the entire complex transfer matrix must be measured (i.e., $N \times N$ measurements) and analysis of this matrix can determine the linear properties of the fiber such as MDL, crosstalk (XT), and gain. Proposed methods such as swept wavelength interferometry for measuring the transfer matrix of an amplifier requires the use of a pair of mode multiplexers which themselves

47

can introduce MDL and XT and no direct feedback can be inferred in the intermediate assembly steps of the amplifier. The issue becomes more pronounced when the number of modes is increased as the mode multiplexer will typically have more parasitic effects [50].

Digital holography is a powerful technique that does not require a mode de-multiplexer, and therefore can be used to measure the transfer matrix at each section of a device [52] reducing he complexity of the system while providing instant feedback. In this work I present the detailed assembly and characterization of a multimode amplifier supporting up to 45 spatial modes an its characterization using digital holography to measure the transfer matrix and obtain the MDL and XT of the amplifier at each step during the assembly from the MMF input through the mode matched splices and all the way to the multimode output. This amplifier was designed and used for pre-amplified detection after going through a turbulent free space link as reported in [52].
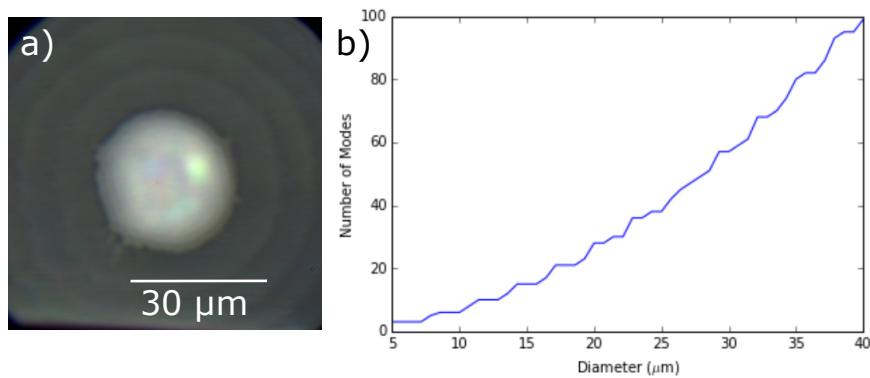
Figure 5.1: a) Microscope Image of the fabricated EDF b) Calculated number of modes supported by the EDF

EDF Fabrication

The step index EDF used for this amplifier was made in house having core and cladding diameters of 30 and 83 μm respectively, with an erbium ion concentration of 4.5×10^{-3} and low refractive index coating with 0.46 NA as shown in Fig. 5.1 (a). The fabrication consist of having a erbium doped rod which is inserted into a silica tube, then a fiber is drawn from this preform. This fiber supports around 60 modes at 1550nm as can be seen in Fig. 5.1 (b), where the number of modes is plotted against the core diameter in the EDF. The relatively core to cladding ratio (30/83) was chosen to increase the pump absorption under cladding pump illumination over a relatively short piece of fiber (2 m). The passive multimode fiber has a graded index profile and is described in [8] supporting 45 spatial modes.The modes of the step index EDF are different than the HG modes in the graded index multimode fiber which causes a high MDL at the splice point. To better match the EDF and graded index multimode fiber we use an intermediate fiber, an 80 μm core diameter graded index fiber having the same mode sizes as that of the 50 μm fiber at 1550 nm, This matching fiber is tapered down to 80 μm cladding diameter to reduce the MDL when spliced to the EDF, after tapering the matching fiber, the mode sizes are a better match to the EDF thus reducing the MDL.

Experimental Setup

The digital holography setup is depicted in Fig. 5.2 (a), light from a tunable laser is split into 2 paths, the first is send to the reference arm and the second is sent into a 1x2 switch for each polarization, and subsequently into a 1x45 switch, which is connected to each of the inputs of a 45-mode multiplexer based on multi-plane light conversion (MPLC) [53]. The MPLC device excites 45 modes into the graded index passive fiber. The output multimode fiber from the MUX

is spliced to 1 m long piece of the 80 μm graded index fiber and subsequently spliced to the EDF after tapering to 80 μm cladding size, which actually matches closely the cladding of the EDF. The tapering process is carried out in a glass processing machine based on CO_2 laser, this taper process is carried out carefully as any ripple/kink during the taper will have a negative impact on the MDL of the fiber. To ensure adiabaticity the fiber is tapered over 2 cm length. The 980-nm pump light from a multimode laser is injected into 2 m of EDF via a coreless fiber which is tapered down to 15 μm and wrapped around the EDF, at the end of the 2m section of EDF a pump dump is used to prevent most of the the unabsorbed pump light to couple into the following passive fiber. Additionally, two dichroic mirrors are used to further reduce the unabsorbed pump light, this will reduce the saturation on the camera, whereas a beam splitter is used to combine the signal and reference beams, and a 4F imaging system is used to record the modes using a InGas camera after passing through a Wollaston prism that allows for simultaneous detection of both polarizations per input polarization. The recorded image shows the interference pattern between the signal and
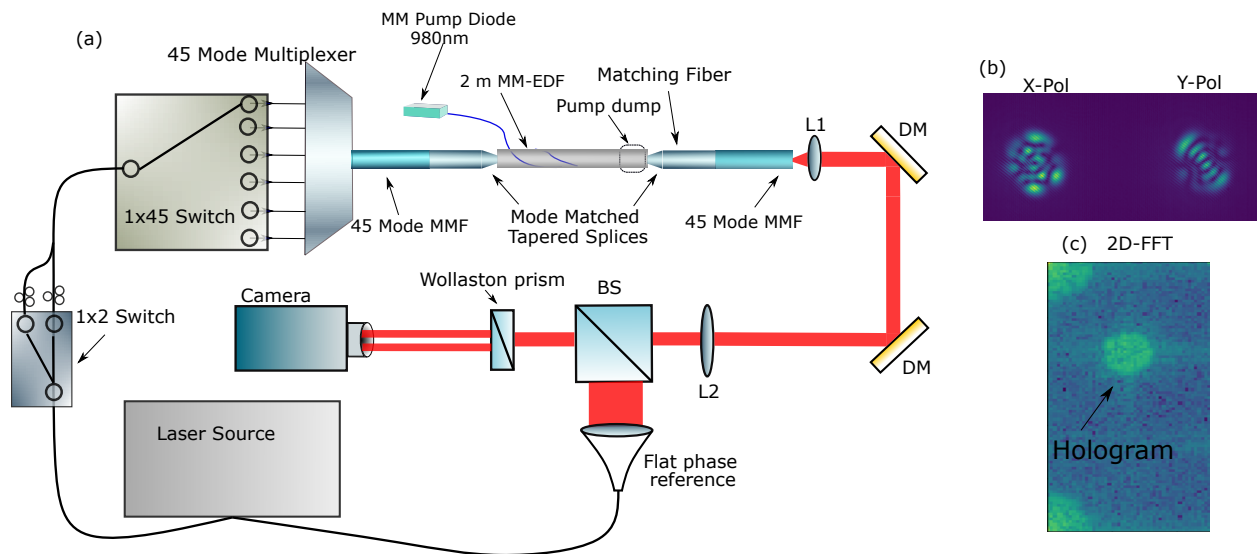
Figure 5.2: (a)Digital holography setup used for the characterization of the MM-EDF amplifier, L1, L2: Lens 1 and 2 respectively, DM: Dichroic mirror, BS: Beam splitter, (b) Captured images on the camera for X and Y polarizations, and (c) resulting hologram.

the reference as seen in Fig. 5.2 (b), after taking the Fourier transform of the recorded image the hologram shown in Fig. 5.2 (c) is obtained.To characterize the whole transfer matrix of the amplifier, we switch over each input mode per polarization and record the amplified mode with the camera.
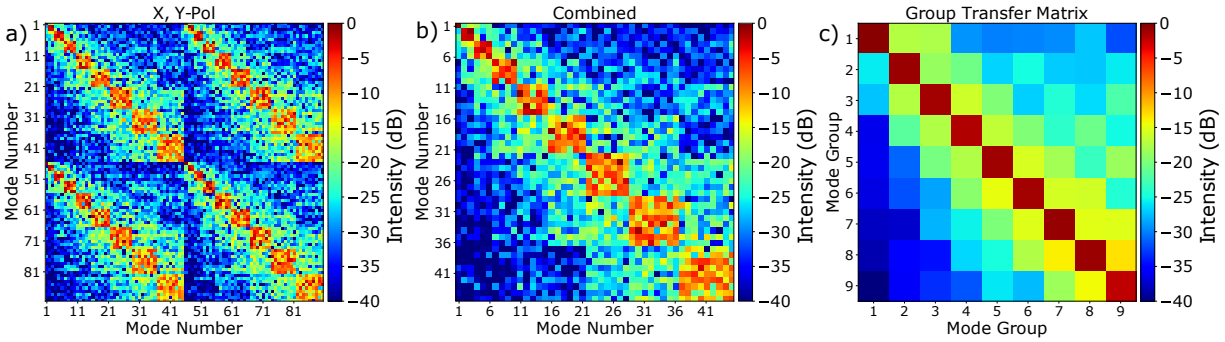
Figure 5.3: Transfer matrices for X and Y polarizations, and summed group transfer matrix after the multimode graded index fiber coupled from the MUX

The holograms are then processed by overlapping with a set of desired modes, for this specific amplifier the first 45 Hermite-Gaussian modes are used as they match closely the eigenmodes of graded-index multimode fiber. Digital holography allows for measuring the whole transfer matrix of the system at each step of the assembly process of the amplifier: the initial transfer matrix is shown in Fig. 5.3 (a) which is the output of the multimode fiber after the MUX, two per polarization transfer matrices that combined form the complete transfer matrix as seen in Fig. 5.3 (b) are obtained, typically showing strong mode coupling within the mode groups, when adding all modes for each mode group the diagonal transfer matrix per mode group can be calculated as shown in Fig. 5.3 (c), where the measured XT from the obtained transfer matrix is around 11-dB. The XT is calculated as the ratio between the total power in the diagonal respect to the power in the non-diagonal area of the transfer matrix.

After splicing the matching fiber one can obtain a new transfer matrix of the system from where

crosstalk and MDL degradation can be obtained, the same case applies after tapering the fiber to match the EDF mode sizes, a new transfer matrix after the taper is measured, this transfer matrix gives information about the taper performance, this taper is performed using a CO_2 glass processing machine, an ideal taper where no ripples or other perturbations are included will be the same as before tapering, in this case we observe degradation in crosstalk and MDL from the transfer matrix due to perturbations along the taper such as ripples. The next step is the splice to EDF after which we can measure the transfer matrix of the system, one should notice that in this case the pump is on to amplify the modes and overcome the absorption of the EDF, we then splice again the matching fiber and 45 mode signal fiber to fully assemble the amplifier. The main characteristic's we are interested in are the XT and MDL of the system which are calculated from the transfer matrix according as performed in [52].

Results and discussion

The use of digital holography allows measure the transfer matrix at each step during the assembly of the amplifier which is not possible otherwise. The transfer matrix after the multimode graded index fiber is used as a reference for the performance of the amplifier when adding/splicing each passive and active fiber. First when splicing the 80 μm fiber the measured transfer matrix is shown in Fig. 5.4 (a), a slight degradation of the XT to 3.3-dB after the splice is observed due to the mode overlap during the splice, Fig. 5.4 (b) shows the transfer matrix after tapering which is almost the same as before tapering with little degradation in XT to 1.75-dB, this process continues and for each splice point the transfer matrix can be quantified. After having the whole transfer matrix of the system is possible to quantify the final MDL and XT of this amplifier, Fig. 5.4 (c) shows the final transfer matrix after the final splice to the multimode fiber in which the measured XT value is -3.2-dB due to the mode mismatch, where the XT for higher order modes is stronger than that of
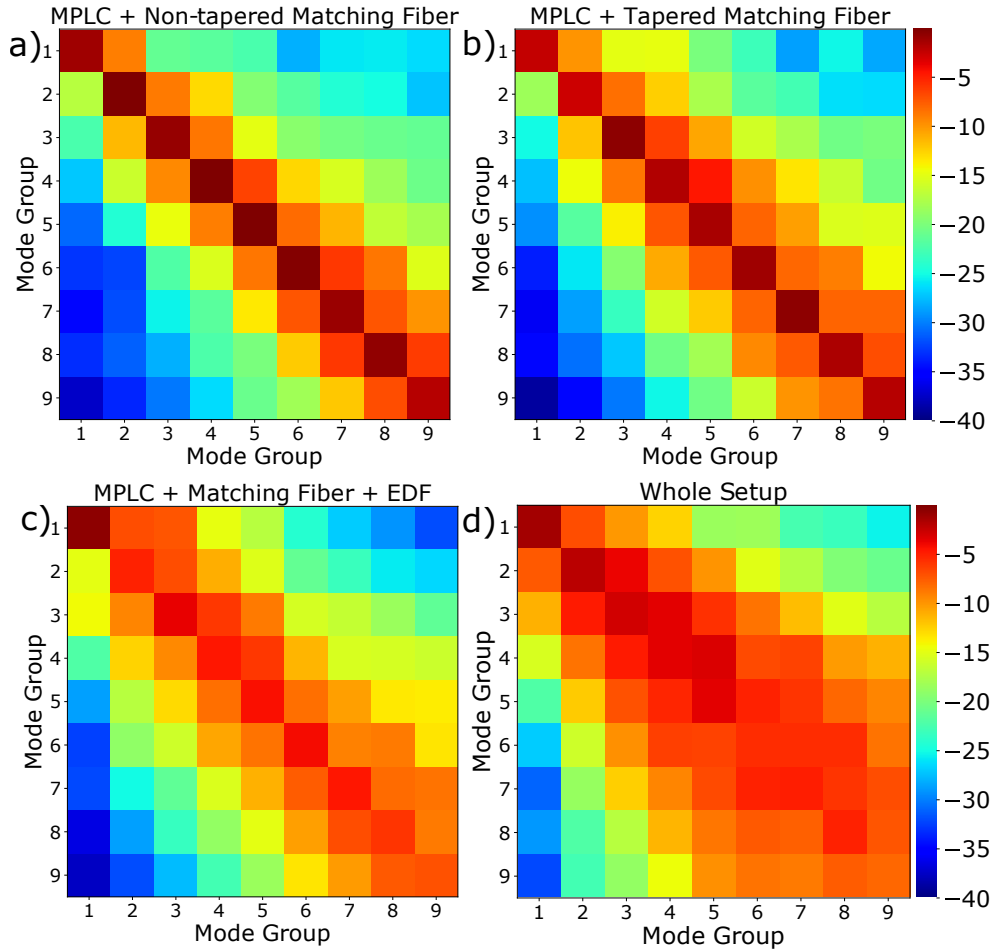
Figure 5.4: Transfer matrices during the assembly process (a) after splicing 80 μm matching fiber, (b) after tapering mode matching fiber(c) after the final multimode fiber spliced to the amplifier

the first mode groups, however, most of the power is confined within the diagonal of the transfer matrix. The method described here allows the measurement of the transfer matrix to quantify the MDL at each step of the assembly, in the reference transfer matrix the measured MDL is only 9.5 dB, after adding each fiber the MDL is degraded and this method can quantify how much is the MDL degraded, when adding the 80 μm fiber the MDL is 11.1-dB, whereas, after tapering the MDL increases to 13.4-dB, at the final transfer matrix the MDL has a value of 16.8-dB. It is

important to notice that this technique allows for an active alignment by monitoring MDL without the need of a second MUX.

Conclusions

In this chapter I have presented an active alignment method that allows the characterization of a multimode EDFA using digital holography, this technique allows for a step by step characterization of the amplifier by measuring the transfer matrix of the system, and obtaining important parameters such as MDL and XT at each splice point while requiring only one single multiplexer, and can be applied regardless of the number of modes. The method presented is proven to be useful for the characterization of active multimode fiber components and allows to have instant feedback to address the amplifier performance.

LIST OF PUBLICATIONS

[JC1] M. Mounaix, N. K. Fontaine, D. T. Neilson, R. Ryf, H. Chen, **Alvarado-Zacarias, Juan Carlos**, and J. Carpenter, "Time reversed optical waves by arbitrary vector spatiotemporal field generation," *Nature Communications*, vol. 11, p. 5813, Nov 2020.

[JC2] N. K. Fontaine, R. Ryf, Y. Zhang, **J. C. Alvarado-Zacarias**, S. van der Heide, M. Mazur, H. Huang, H. Chen, R. Amezcua-Correa, G. Li, M. Capuzzo, R. Kopf, A. Tate, H. Safar, C. Bolle, D. T. Neilson, E. Burrows, K. Kim, M. Bigot-Astruc, F. Achten, P. Sillard, A. Amezcua-Correa, and J. Carpenter, "Digital turbulence compensation of free space optical link with multimode optical amplifier," in *45th European Conference on Optical Communication (ECOC 2019)*, pp. 1–4, 2019.

[JC3] D. Cruz-Delgado, **Alvarado-Zacarias, JC**, H. Cruz-Ramirez, J. Antonio-Lopez, S. Leon-Saval, R. Amezcua-Correa, and A. U'Ren, "Control over the transverse structure and long-distance fiber propagation of light at the single-photon level," *Scientific reports*, vol. 9, no. 1, pp. 1–9, 2019.

[JC4] Y. Huang, H. Chen, H. Huang, Z. Li, N. K. Fontaine, R. Ryf, **Alvarado, Juan Carlos**, R. Amezcua-Correa, J. van Weerdenburg, C. Okonkwo, *et al.*, "Mode-and wavelength-multiplexed transmission with crosstalk mitigation using a single amplified spontaneous emission source," *Photonics Research*, vol. 7, no. 11, pp. 1363–1369, 2019.

[JC5] R. Amezcua-Correa, S. Leon-Saval, Z. Sanjabi Eznaveh, J. Enrique Antonio-Lopez, **Carlos Alvarado Zacarias, Juan**, G. Milione, K. Shi, B. Thomsen, D. Richardson, and Y. Jung, "Generation of orbital angular momentum beams using all-fiber photonic lanterns," 2018.

[JC6] H. Liu, B. Huang, **Zacarias, Juan Carlos Alvarado**, H. Wen, H. Chen, N. K. Fontaine, R. Ryf, J. E. Antonio-Lopez, R. A. Correa, and G. Li, "Turbulence-resistant fso communication using a few-mode pre-amplified receiver," *Scientific reports*, vol. 9, no. 1, pp. 1–7, 2019.

[JC7] H. Chen, **Alvarado-Zacarias, Juan Carlos**, H. Huang, N. K. Fontaine, R. Ryf, D. T. Neilson, and R. Amezcua-Correa, "Mode-multiplexed full-field reconstruction using direct and phase retrieval detection," in *Optical Fiber Communication Conference*, pp. W4A–5, Optical Society of America, 2020.

[JC8] N. Wang, I. Kim, O. Vassilieva, T. Ikeuchi, H. Wen, J. Antonio-Lopez, **Alvarado-Zacarias, JC**, H. Liu, S. Fan, M. S. Habib, *et al.*, "Low-crosstalk few-mode edfas using retro-reflection for single-mode fiber trunk lines and networks," *Optics Express*, vol. 27, no. 24, pp. 35962–35970, 2019.

[JC9] R. Veronese, **Zacarias, Juan Carlos Alvarado**, S. van der Heide, R. Amezcua-Correa, H. Chen, R. Ryf, N. K. Fontaine, M. Santagiustina, A. Galtarossa, and L. Palmieri, "Distributed supermode coupling measurements in multi-core optical fibers," in *2020 Optical Fiber Communications Conference and Exhibition (OFC)*, pp. 1–3, IEEE, 2020.

[JC10] Y. Liu, G. Yang, N. Wang, L. Ma, **Alvarado-Zacarias, JC**, J. E. Antonio-Lopez, P. Sillard, A. Amezcua-Correa, R. Amezcua-Correa, X. Fan, *et al.*, "Investigation of brillouin dynamic grating in 4-lp-mode fiber with a ring-cavity configuration for distributed temperature and strain sensing application," in *2020 Optical Fiber Communications Conference and Exhibition (OFC)*, pp. 1–3, IEEE, 2020.

[JC11] R.-J. Essiambre, R. Ryf, S. van der Heide, J. I. Bonetti, H. Huang, M. Kodialam, F. J. García-Gómez, E. C. Burrows, **Alvarado-Zacarias, Juan C**, R. Amezcua-Correa, *et al.*,

"First transmission of a 12d format across three coupled spatial modes of a 3-core coupled-core fiber at 4 bits/s/hz," in *2020 Optical Fiber Communications Conference and Exhibition (OFC)*, pp. 1–3, IEEE, 2020.

[JC12] S. van der Heide, **Alvarado-Zacarias, Juan Carlos**, N. K. Fontaine, R. Ryf, H. Chen, R. Amezcua-Correa, T. Koonen, and C. Okonkwo, "Low-loss low-mdl core multiplexer for 3-core coupled-core multi-core fiber," in *2020 Optical Fiber Communications Conference and Exhibition (OFC)*, pp. 1–3, IEEE, 2020.

[JC13] Y. Liu, G. Yang, N. Wang, L. Ma, **Alvarado-Zacarias, JC**, J. Antonio-Lopez, P. Sillard, A. Amezcua-Correa, R. Amezcua-Correa, X. Fan, *et al.*, "Observation on temperature and strain dependency of brillouin dynamic grating in a few-mode fiber with a ring-cavity configuration," *Optics Letters*, vol. 45, no. 8, pp. 2152–2155, 2020.

[JC14] **Alvarado-Zacarias, Juan Carlos**, N. K. Fontaine, R. Ryf, H. Chen, S. van der Heide, J. E. Antonio-Lopez, S. Wittek, G. Li, C. Okonkwo, M. Bigot-Astruc, *et al.*, "Assembly and characterization of a multimode edfa using digital holography," in *Optical Fiber Communication Conference*, pp. Th1H–6, Optical Society of America, 2020.

[JC15] N. Wang, **Alvarado-Zacarias, JC**, M. S. Habib, H. Wen, J. Antonio-Lopez, P. Sillard, A. Amezcua-Correa, A. Schülzgen, R. Amezcua-Correa, and G. Li, "Mode-selective few-mode brillouin fiber lasers based on intramodal and intermodal sbs," *Optics Letters*, vol. 45, no. 8, pp. 2323–2326, 2020.

[JC16] H. Chen, N. K. Fontaine, Y. Zhang, M. Mazur, **Alvarado-Zacarias, Juan Carlos**, R. Ryf, D. T. Neilson, G. Li, R. Amezcua-Correa, and J. Carpenter, "Optical broadcasting and steering by demultiplexing incoherent spatial modes," in *Optical Fiber Communication Conference*, pp. Th4B–7, Optical Society of America, 2020.

[JC17] C. Matte-Breton, R. Ryf, N. K. Fontaine, R.-J. Essiambre, H. Chen, Y. Messaddeq, **Zacarias, Juan Carlos Alvarado**, R. A. Correa, C. Kelly, and S. LaRochelle, "An 8-core erbium-doped fiber with annular doping for low gain compression in cladding-pumped amplifiers," in *45th European Conference on Optical Communication (ECOC 2019)*, pp. 1–3, IET, 2019.

[JC18] **Alvarado-Zacarias, Juan Carlos**, J. E. Antonio-Lopez, N. K. Fontaine, A. Amezcua-Correa, P. Sillard, M. Bigot-Astruc, M. Jansen, S. G. Leon-Saval, G. Li, and R. Amezcua-Correa, "7-core× 6-mode photonic lantern mode multiplexer," in *45th European Conference on Optical Communication (ECOC 2019)*, pp. 1–4, IET, 2019.

[JC19] S. Eikenberry, A. Gonzalez, A. Townsend, S. Jeram, R. Amezcua-Correa, **Alvarado-Zacarias, J**, C. Moraitis, J. Harrington, T. Maccarone, M. Bentz, *et al.*, "Polyoculus: Low-cost spectroscopy for the community," in *American Astronomical Society Meeting Abstracts# 236*, vol. 236, pp. 311–02, 2020.

[JC20] **Alvarado-Zacarias, Juan Carlos**, N. K. Fontaine, R. Ryf, H. Chen, P. Sillard, and R. Amezcua-Correa, "Components and amplifiers for space division multiplexing," in *2020 IEEE Photonics Society Summer Topicals Meeting Series (SUM)*, pp. 1–2, IEEE, 2020.

[JC21] M. Mounaix, N. K. Fontaine, D. T. Neilson, R. Ryf, H. Chen, **Alvarado-Zacarias, Juan Carlos**, and J. Carpenter, "Optical time reverser," in *CLEO: Science and Innovations*, pp. SM2H–7, Optical Society of America, 2020.

[JC22] R. Sampson, F. G. Vanani, Y. Zhang, H. Liu, A. Fardoost, N. Wang, H. Wen, **Alvarado-Zacarias, Juan Carlos**, R. A. Correa, and G. Li, "Turbulence-resistant free-space optical communications using few-mode dpsk," in *CLEO: QELS_Fundamental Science*, pp. JTu2E–2, Optical Society of America, 2020.

[JC23] H. Chen, N. K. Fontaine, **Alvarado-Zacarias, Juan Carlos**, C. Cheng, M. Bigot, P. Sillard, R. Ryf, M. Mazur, D. T. Neilson, R. Amezcua-Correa, *et al.*, "Multiport swept-wavelength interferometer with laser phase noise mitigation employing a broadband ultra-weak fbg array," *Optics Letters*, vol. 45, no. 21, pp. 5913–5916, 2020.

[JC24] M. Mounaix, N. K. Fontaine, D. T. Neilson, H. Chen, R. Ryf, **Alvarado-Zacarias, JC**, and J. Carpenter, "Full polarization-resolved spatiotemporal beam shaping," in *Conference on Lasers and Electro-Optics/Pacific Rim*, p. C3B_2, Optical Society of America, 2020.

[JC25] N. Wang, I. Kim, O. Vassilieva, T. Ikeuchi, H. Wen, J. E. Antonio-Lopez, **J. C. Alvarado-Zacarias**, H. Liu, S. Fan, M. S. Habib, R. Amezcua-Correa, and G. Li, "Low-crosstalk few-mode edfas using retro-reflection for single-mode fiber trunk lines and networks," *Opt. Express*, vol. 27, pp. 35962–35970, Nov 2019.

[JC26] H. Liu, B. Huang, **Juan Carlos Alvarado Zacarias**, H. Wen, H. Chen, N. K. Fontaine, R. Ryf, J. E. Antonio-Lopez, R. A. Correa, and G. Li, "Turbulence-resistant fso communication using a few-mode pre-amplified receiver," *Scientific Reports*, vol. 9, no. 1, p. 16247, 2019.

[JC27] Y. Huang, H. Chen, H. Huang, Z. Li, N. K. Fontaine, R. Ryf, **Juan Carlos Alvarado**, R. Amezcua-Correa, J. van Weerdenburg, C. Okonkwo, A. M. J. Koonen, Y. Song, and M. Wang, "Mode- and wavelength-multiplexed transmission with crosstalk mitigation using a single amplified spontaneous emission source," *Photon. Res.*, vol. 7, pp. 1363–1369, Nov 2019.

[JC28] D. Cruz-Delgado, **Alvarado-Zacarias, J. C.**, H. Cruz-Ramirez, J. E. Antonio-Lopez, S. G. Leon-Saval, R. Amezcua-Correa, and A. B. U'Ren, "Control over the transverse structure and long-distance fiber propagation of light at the single-photon level," *Scientific Reports*, vol. 9, no. 1, p. 9015, 2019.

[JC29] N. Wang, **J.C. Alvarado**, M. S. Habib, H. Wen, Y. Zhang, J. E. Antonio-Lopez, P. Sillard, A. Amezcua-Correa, R. Amezcua-Correa, and G. Li, "High-order mode brillouin fiber lasers based on intra- and inter-modal sbs," in *Conference on Lasers and Electro-Optics*, p. SM1L.1, Optical Society of America, 2019.

[JC30] R. Ryf, N. K. Fontaine, S. Wittek, K. Choutagunta, M. Mazur, H. Chen, and **Juan Carlos Alvarado-Zacarias**, "Recent advances in mode-multiplexed transmission over multimode fibers," in *Conference on Lasers and Electro-Optics*, p. SM1G.1, Optical Society of America, 2019.

[JC31] Y. Huang, H. Chen, H. Huang, Y. Song, Z. Li, N. K. Fontaine, R. Ryf, **Juan Carlos Alvarado**, R. Amezcua-Correa, and M. Wang, "Mode-multiplexed transmission with crosstalk mitigation using amplified spontaneous emission (ase)," in *Conference on Lasers and Electro-Optics*, p. SM1G.2, Optical Society of America, 2019.

[JC32] K. Choutagunta, R. Ryf, N. Fontaine, S. Wittek, **J. C. Alvarado-Zacarias**, M. Mazur, H. Chen, R. Essiambre, R. Amezcua-Correa, T. Hayashi, Y. Tamura, T. Hasegawa, T. Taru, and J. M. Kahn, "Modal dynamics in spatially multiplexed links," in *2019 Optical Fiber Communications Conference and Exhibition (OFC)*, pp. 1–3, March 2019.

[JC33] **J. C. Alvarado-Zacarias**, J. E. Antonio-Lopez, M. S. Habib, S. Gausmann, N. Wang, D. Cruz-Delgado, A. Schulzgen, A. Amezcua-Correa, L. Demontmorillon, P. Sillard, and R. Amezcua-Correa, "Low-loss 19 core fan-in/fan-out device using reduced-cladding graded index fibers," in *2019 Optical Fiber Communications Conference and Exhibition (OFC)*, pp. 1–3, March 2019.

[JC34] N. Wang, I. Kim, O. Vassilieva, T. Ikeuchi, H. Wen, J. E. Antonio-Lopez, **J. C. Alvarado-Zacarias**, P. Sillard, C. Gonnet, H. Liu, S. Fan, M. S. Habib, R. Amezcua-Correa, and G. Li, "Low-crosstalk few-mode edfa for single-mode fiber trunk lines and networks," in *Optical*

Fiber Communication Conference (OFC) 2019, p. Th1B.4, Optical Society of America, 2019.

[JC35] S. Wittek, R. Ryf, N. K. Fontaine, K. Choutagunta, M. Mazur, H. Chen, **Juan Carlos Alvarado-Zacarias**, M. Capuzzo, R. Kopf, A. Tate, H. Safar, C. Bolle, D. T. Neilson, E. Burrows, K. Kim, M. Bigot-Astruc, F. Achten, P. Sillard, A. Amezcua-Correa, J. M. Kahn, J. Schröder, R. Amezcua-Correa, and J. Carpenter, "Mode-multiplexed transmission within and across mode groups of a multimode-fiber," in *Optical Fiber Communication Conference (OFC) 2019*, p. M2I.2, Optical Society of America, 2019.

[JC36] **Juan Carlos Alvarado-Zacarias**, C. Matte-Breton, R. Ryf, N. K. Fontaine, H. Chen, S. Wittek, H. Sakuma, T. Ohtsuka, T. Hayashi, T. Hasegawa, S. LaRochelle, and R. Amezcua-Correa, "Characterization of coupled-core fiber amplifiers using swept-wavelength interferometer," in *Optical Fiber Communication Conference (OFC) 2019*, p. Th1B.6, Optical Society of America, 2019.

[JC37] R. Sampson, H. Liu, X. Su, B. Huang, **Juan Carlos Alvarado Zacarias** , T. Zhan, R. A. Correa, and G. Li, "Turbulence-resistant free-space communication using few-mode pre-amplifiers," in *Next-Generation Optical Communication: Components, Sub-Systems, and Systems VIII* (G. Li and X. Zhou, eds.), vol. 10947, pp. 29 – 35, International Society for Optics and Photonics, SPIE, 2019.

[JC38] N. Wang, **J. C. Alvarado Zacarias**, J. E. Antonio-Lopez, Z. S. Eznaveh, C. Gonnet, P. Sillard, S. Leon-Saval, A. Schülzgen, G. Li, and R. Amezcua-Correa, "Transverse mode-switchable fiber laser based on a photonic lantern," *Opt. Express*, vol. 26, pp. 32777–32787, Dec 2018.

[JC39] Z. S. Eznaveh, **Juan Carlos Alvarado Zacarias** , J. E. A. Lopez, K. Shi, G. Milione, Y. Jung, B. C. Thomsen, D. J. Richardson, N. Fontaine, S. G. Leon-Saval, and R. A. Correa,

"Photonic lantern broadband orbital angular momentum mode multiplexer," *Opt. Express*, vol. 26, pp. 30042–30051, Nov 2018.

[JC40] R. Ryf, N. K. Fontaine, S. Wittek, K. Choutagunta, M. Mazur, H. Chen, **J. Carlos Alvarado-Zacarias**, R. Amezcua-Correa, M. Capuzzo, R. Kopf, A. Tate, H. Safar, C. Bolle, D. T. Neilson, E. Burrows, K. Kim, M. Bigot-Astruc, F. Achten, P. Sillard, A. Amezcua-Correa, J. M. Kahn, J. Schröder, and J. Carpenter, "High-spectral-efficiency mode-multiplexed transmission over graded-index multimode fiber," in *2018 European Conference on Optical Communication (ECOC)*, pp. 1–3, Sep. 2018.

[JC41] S. van der Heide, J. van Weerdenburg, M. Biqot-Astruc, A. Amezcua-Correa, J. Antonio-Lopez, **J. C. Alvarado-Zacarias**, H. de Waardt, T. Koenen, P. Sillard, R. Amezcua-Correa, and C. Okonkwo, "Single carrier 1 tbit/s mode-multiplexed transmission over graded-index 50 μm core multi-mode fiber employing kramers-kronig receivers," in *2018 European Conference on Optical Communication (ECOC)*, pp. 1–3, Sep. 2018.

[JC42] N. K. Fontaine, R. Ryf, H. Chen, S. Wittek, J. Li, **J. C. Alvarado**, J. E. A. Lopez, M. Cappuzzo, R. Kopf, A. Tate, H. Safar, C. Bolle, D. T. Neilson, E. Burrows, K. W. Kim, P. Sillard, F. Achten, M. Bigot, A. Amezcua-Correa, R. A. Correa, J. Du, Z. He, and J. Carpenter, "Packaged 45-mode multiplexers for a $50 - \mu$m graded index fiber," in *2018 European Conference on Optical Communication (ECOC)*, pp. 1–3, Sep. 2018.

[JC43] H. Chen, N. K. Fontaine, R. Ryf, D. T. Neilson, P. Winzer, S. Gross, N. Riesen, M. Withford, J. Li, **J. C. Alvarado**, S. Wittek, J. Du, Z. He, J. E. Antonio Lopez, and R. Amezcua-Correa, "Remote mode-forming over multimode fiber employing single-ended channel estimation," in *2018 European Conference on Optical Communication (ECOC)*, pp. 1–3, Sep. 2018.

[JC44] R. Ryf, N. K. Fontaine, H. Chen, S. Wittek, J. Li, **J. C. Alvarado-Zacarias**, R. Amezcua-Correa, J. E. Antonio-Lopez, M. Capuzzo, R. Kopf, A. Tate, H. Safar, C. Bolle, D. T. Neilson, E. Burrows, K. Kim, M. Bigot-Astruc, F. Achten, P. Sillard, A. Amezcua-Correa, J. Du, Z. He, and J. Carpenter, "Mode-multiplexed transmission over 36 spatial modes of a graded-index multimode fiber," in *2018 European Conference on Optical Communication (ECOC)*, pp. 1–3, Sep. 2018.

[JC45] R. Sampson, H. Liu, H. Wen, Y. Zhang, R. Stegeman, P. Zhang, B. Huang, N. Wang, S. Fan, **Juan C. Alvarado Zacarias**, R. A. Correa, and G. Li, "Improving the sensitivity of lidars using few-mode pre-amplified receivers," in *Frontiers in Optics / Laser Science*, p. FW7A.2, Optical Society of America, 2018.

[JC46] S. Wittek, R. Ryf, N. K. Fontaine, H. Chen, **J. C. Alvarado-Zacarias**, J. Li, J. E. Antonio-Lopez, M. Capuzzo, R. Kopf, A. Tate, H. Safar, C. Bolle, D. T. Neilson, E. Burrows, K. Kim, M. Bigot, A. Amezcua-Correa, P. Sillard, J. Carpenter, and R. Amezcua-Correa, "6th mode-group multiplexer for intra-mode transmission over 50-m gi-multimode fiber," in *2018 IEEE Photonics Society Summer Topical Meeting Series (SUM)*, pp. 25–26, July 2018.

[JC47] **J. C. Alvarado-Zacarias**, N. K. Fontaine, H. Chen, J. E. Antonio-Lopez, R. Ryf, S. Wittek, H. Sakuma, T. Hasegawa, T. Nakanishi, T. Hayashi, and R. Amezcua-Correa, "Cladding-pumped coupled-core edfa," in *2018 IEEE Photonics Society Summer Topical Meeting Series (SUM)*, pp. 263–264, July 2018.

[JC48] J. E. Antonio-Lopez, Z. S. Eznaveh, **J. C. Alvarado-Zacarias**, P. Sillard, A. Amezcua-Correa, C. Gonnet, M. Bigot-Astruc, N. K. Fontaine, R. Ryf, H. Chen, A. Schülzgen, and R. Amezcua-Correa, "Multimode and coupled-core fiber amplifiers," in *2018 IEEE Photonics Society Summer Topical Meeting Series (SUM)*, pp. 259–259, July 2018.

[JC49] J. E. Antonio-Lopez, **J. Carlos Alvarado-Zacarias**, Z. Sanjabi-Eznaveh, P. Sillard, A. Amezcua-Correa, C. Gonnet, M. Bigot-Astruc, N. K. Fontaine, R. Ryf, H. Chen, and R. Amezcua-Correa, "Multimode and coupled-core fiber amplifiers for sdm," in *2018 23rd Opto-Electronics and Communications Conference (OECC)*, pp. 1–2, July 2018.

[JC50] A. M. Velázquez-Benítez, J. E. Antonio-López, **Alvarado-Zacarías, Juan C.**, N. K. Fontaine, R. Ryf, H. Chen, J. Hernández-Cordero, P. Sillard, C. Okonkwo, S. G. Leon-Saval, and R. Amezcua-Correa, "Scaling photonic lanterns for space-division multiplexing," *Scientific Reports*, vol. 8, no. 1, p. 8897, 2018.

[JC51] B. Huang, **Juan Carlos Alvarado Zacarias**, H. Liu, N. K. Fontaine, H. Chen, R. Ryf, F. Poletti, J. R. Hayes, J. Antonio-Loppez, J. Zhao, R. A. Correa, and G. Li, "Triple-clad photonic lanterns for mode scaling," *Opt. Express*, vol. 26, pp. 13390–13396, May 2018.

[JC52] M. Parto, H. Lopez-Aviles, J. E. Antonio-Lopez, **J. C. Alvarado Zacarias**, M. Khajavikhan, R. Amezcua-Correa, and D. N. Christodoulides, "Observation of aharonov-bohm suppression of optical tunneling in twisted multicore fibers," in *Conference on Lasers and Electro-Optics*, p. FM1E.2, Optical Society of America, 2018.

[JC53] R. Amezcua-Correa, J. E. Antonio-Lopez, Z. S. Eznaveh, **Juan Carlos Alvarado Zacarias**, A. Schülzgen, G. Li, N. Fontaine, R. Ryf, H. Chen, C. Gonnet, and P. Sillard, "Low-differential modal gain multimode fiber amplifiers (Conference Presentation)," in *Next-Generation Optical Communication: Components, Sub-Systems, and Systems VII* (G. Li and X. Zhou, eds.), vol. 10561, International Society for Optics and Photonics, SPIE, 2018.

[JC54] J. van Weerdenburg, R. Ryf, **Juan Carlos Alvarado-Zacarias**, R. A. Alvarez-Aguirre, N. K. Fontaine, H. Chen, R. Amezcua-Correa, Y. Sun, L. Grüner-Nielsen, R. V. Jensen,

R. Lingle, T. Koonen, and C. Okonkwo, "138-tb/s mode- and wavelength-multiplexed transmission over six-mode graded-index fiber," *J. Lightwave Technol.*, vol. 36, pp. 1369–1374, Mar 2018.

[JC55] **Juan Carlos Alvarado-Zacarias**, N. K. Fontaine, H. Chen, J. E. Antonio-Lopez, S. Wittek, J. Li, S. Gausmann, R. Ryf, C. Gonnet, A. Amezcua-Correa, M. Bigot, A. Schülzgen, G. Li, P. Sillard, and R. Amezcua-Correa, "Coupled-core edfa compatible with fmf transmission," in *Optical Fiber Communication Conference Postdeadline Papers*, p. Th4A.3, Optical Society of America, 2018.

[JC56] H. Liu, H. Wen, **Juan Carlos Alvarado Zacarias**, J. E. Antonio-Lopez, N. Wang, P. Sillard, R. Amezcua-Correa, and G. Li, "Demonstration of stable 3x10 gb/s mode group-multiplexed transmission over a 20 km few-mode fiber," in *Optical Fiber Communication Conference*, p. W4J.2, Optical Society of America, 2018.

[JC57] J. van Weerdenburg, R. Ryf, R. Alvarez-Aguirre, N. K. Fontaine, R. Essiambre, H. Chen, **J. C. Alvarado-Zacarias**, R. Amezcua-Correa, S. Gross, N. Riesen, M. Withford, D. W. Peckham, A. McCurdy, R. Lingle, T. Koonen, and C. Okonkwo, "Mode-multiplexed 16-qam transmission over 2400-km large-effective-area depressed-cladding 3-mode fiber," in *2018 Optical Fiber Communications Conference and Exposition (OFC)*, pp. 1–3, March 2018.

[JC58] H. Chen, N. K. Fontaine, R. Ryf, **J. C. Alvarado**, J. van Weerdenburg, R. Amezcua-Correa, C. Okonkwo, and T. Koonen, "Optical crosstalk reduction using amplified spontaneous emission (ase)," in *2018 Optical Fiber Communications Conference and Exposition (OFC)*, pp. 1–3, March 2018.

[JC59] **J. C. Alvarado-Zacarias**, N. K. Fontaine, J. E. Antonio-Lopez, Z. S. Eznaveh, M. S. Habib, H. Chen, R. Ryf, D. Van Ras, P. Sillard, C. Gonnet, A. Amezcua-Correa, S. G.

Leon-Saval, and R. A. Correa, "Mode selective photonic lantern with graded index core," in *2018 Optical Fiber Communications Conference and Exposition (OFC)*, pp. 1–3, March 2018.

[JC60] R. Ryf, J. van Weerdenburg, R. A. Alvarez-Aguirre, N. K. Fontaine, R.-J. Essiambre, H. Chen, **Juan Carlos Alvarado-Zacarias**, R. Amezcua-Correa, T. Koonen, and C. Okonkwo, "White gaussian noise based capacity estimate and characterization of fiber-optic links," in *Optical Fiber Communication Conference*, p. W1G.2, Optical Society of America, 2018.

[JC61] N. K. Fontaine, H. Chen, R. Ryf, **Juan Carlos Alvarado-Zacarias**, Z. S. Eznaveh, J. E. Antonio-Lopez, and R. A. Correa, "Multimode and multi-core fiber amplifiers for space-division multiplexed communications systems," in *Asia Communications and Photonics Conference*, p. M1J.4, Optical Society of America, 2017.

[JC62] B. Huang, C. Carboni, H. Liu, **J. C. Alvarado-Zacarias**, F. Peng, Y. Lee, H. Chen, N. K. Fontaine, R. Ryf, J. E. Antonio-Lopez, R. Amezcua-Correa, and G. Li, "Turbulence-resistant free-space optical communication using few-mode preamplified receivers," in *2017 European Conference on Optical Communication (ECOC)*, pp. 1–3, Sep. 2017.

[JC63] R. Ryf, N. K. Fontaine, S. H. Chang, **J. C. Alvarado**, B. Huang, J. Antonio-López, H. Chen, R. Essiambre, E. Burrows, R. W. Tkach, R. Amezcua-Correa, T. Hayashi, Y. Tamura, T. Hasegawa, and T. Taru, "Long-haul transmission over multi-core fibers with coupled cores," in *2017 European Conference on Optical Communication (ECOC)*, pp. 1–3, Sep. 2017.

[JC64] R. Ryf, N. K. Fontaine, S. H. Chang, **J. C. Alvarado**, B. Huang, J. Antonio-López, H. Chen, R. Essiambre, E. Burrows, R. W. Tkach, R. Amezcua-Correa, T. Hayashi, Y. Tamura, T. Hasegawa, and T. Taru, "Long-haul transmission over multi-core fibers with

coupled cores," in *2017 European Conference on Optical Communication (ECOC)*, pp. 1–3, Sep. 2017.

[JC65] N. K. Fontaine, H. Chen, R. Ryf, D. Neilson, **J. C. Alvarado**, J. van Weerdenburg, R. Amezcua-Correa, C. Okonkwo, and J. Carpenter, "Programmable vector mode multiplexer," in *2017 European Conference on Optical Communication (ECOC)*, pp. 1–3, Sep. 2017.

[JC66] J. van Weerdenburg, R. Ryf, **J. C. Alvarado-Zacarias**, R. A. Alvarez-Aguirre, N. K. Fontaine, H. Chen, R. Amezcua-Correa, T. Koonen, and C. Okonkwo, "138 tbit/s transmission over 650 km graded-index 6-mode fiber," in *2017 European Conference on Optical Communication (ECOC)*, pp. 1–3, Sep. 2017.

[JC67] Y. Jung, Q. Kang, L. Shen, S. Chen, H. Wang, Y. Yang, K. Shi, B. C. Thomsen, R. A. Correa, Z. S. Eznaveh, **J. C. Alvarado Zacarias**, J. Antonio-Lopez, P. Barua, J. K. Sahu, S. U. Alam, and D. J. Richardson, "Few mode ring-core fibre amplifier for low differential modal gain," in *2017 European Conference on Optical Communication (ECOC)*, pp. 1–3, Sep. 2017.

[JC68] K. Shi, Y. Jung, Z. S. Eznaveh, **J. C. Alvarado Zacarias**, J. E. A. Lopez, H. Zhou, R. Zhang, S. Chen, H. Wang, Y. Yang, R. A. Correa, D. J. Richardson, and B. C. Thomsen, "10×10 mdm transmission over 24 km of ring-core fibre using mode selective photonic lanterns and sparse equalization," in *2017 European Conference on Optical Communication (ECOC)*, pp. 1–3, Sep. 2017.

[JC69] M. Blau, M. Rosenfeld, **Juan Carlos Alvarado Zacarias**, R. A. Correa, and D. M. Marom, "Broadband mode-group mixing via spatial phase masks printed on fiber facet," in *Advanced Photonics 2017 (IPR, NOMA, Sensors, Networks, SPPCom, PS)*, p. NeW3B.3, Optical Society of America, 2017.

[JC70] J. E. Antonio-Lopez, Z. S. Eznaveh, **J. C. Alvarado-Zacarias**, R. Ryf, N. K. Fontaine, A. Schülzgen, and R. A. Correa, "Space division multiplexing fibers and amplifiers," in *Advanced Photonics 2017 (IPR, NOMA, Sensors, Networks, SPPCom, PS)*, p. NeW3B.1, Optical Society of America, 2017.

[JC71] Z. S. Eznaveh, J. E. Antonio-Lopez, **J. C. Alvarado Zacarias**, A. Schülzgen, C. M. Okonkwo, and R. A. Correa, "All-fiber few-mode multicore photonic lantern mode multiplexer," *Opt. Express*, vol. 25, pp. 16701–16707, Jul 2017.

[JC72] M. S. Habib, J. E. Antonio-Lopez, A. V. Newkirk, **Juan Carlos Alvarado Zacarias**, A. Schülzgen, R. Amezuca-Correa, C. Markos, O. Bang, and M. Bache, "Toward single-mode uv to near-ir guidance using hollow-core anti-resonant silica fiber," in *2017 European Conference on Lasers and Electro-Optics and European Quantum Electronics Conference*, pp. 10–14, Optical Society of America, 2017.

[JC73] N. Wang, Z. S. Eznaveh, **J. C. Alvarado Zacarias**, J. E. Antonio-Lopez, S. Leon-Saval, P. Sillard, C. Gonnet, A. Schülzgen, G. Li, and R. Amezcua-Correa, "Erbium-doped fiber amplifier for oam modes using an annular-core photonic lantern," in *Conference on Lasers and Electro-Optics*, p. STu4K.4, Optical Society of America, 2017.

[JC74] M. A. Eftekhar, Z. Sanjabi-Eznaveh, J. E. Antonio-Lopez, **J. C. Alvarado Zacarias**, A. Schülzgen, M. Kolesik, F. W. Wise, R. A. Correa, and D. N. Christodoulides, "Broadband supercontinuum generation in tapered multimode graded-index optical fibers," in *Conference on Lasers and Electro-Optics*, p. STh1K.7, Optical Society of America, 2017.

[JC75] D. Cruz-Delgado, **J.C. Alvarado-Zacarias**, H. Cruz-Ramirez, J. Antonio-Lopez, S. G. Leon-Saval, R. Amezcua-Correa, and A. B. U'Ren, "Deterministic transverse mode conversion at the single-photon level," in *Conference on Lasers and Electro-Optics*, p. STh1K.3, Optical Society of America, 2017.

[JC76] N. K. Fontaine, J. E. A. Lopez, H. Chen, R. Ryf, D. Neilson, A. Schulzgen, **Juan Carlos Alvarado Zacarias**, R.-J. Essiambre, H. Sakuma, T. Hasegawa, T. Nakanishi, T. Hayashi, and R. Amezcua-Correa, "Coupled-core optical amplifier," in *Optical Fiber Communication Conference Postdeadline Papers*, p. Th5D.3, Optical Society of America, 2017.

[JC77] Z. S. Eznaveh, **J. C. Alvarado Zacarias**, J. E. A. Lopez, Y. Jung, K. Shi, B. C. Thomsen, D. J. Richardson, S. Leon-Saval, and R. A. Correa, "Annular core photonic lantern oam mode multiplexer," in *Optical Fiber Communication Conference*, p. Tu3J.3, Optical Society of America, 2017.

[JC78] H. Liu, H. W. and**Juan Carlos Alvarado Zacarias**, J. E. Antonio-Lopez, N. Wang, P. Sillard, A. A. Correa, R. Amezcua-Correa, and G. Li, "3×10 gb/s mode group-multiplexed transmission over a 20 km few-mode fiber using photonic lanterns," in *Optical Fiber Communication Conference*, p. M2D.5, Optical Society of America, 2017.

[JC79] H. Chen, B. Huang, N. K. Fontaine, R. Ryf, **J. C. Alvarado**, Z. S. Eznaveh, A. Schiilzgen, P. Sillard, C. Gonnet, J. E. A. Lopez, G. Li, and R. Amezcua-Correa, "Mode-dependent gain characterization of erbium-doped multimode fiber using c2 imaging," in *2017 Optical Fiber Communications Conference and Exhibition (OFC)*, pp. 1–3, March 2017.

[JC80] B. Huang, **J.C. Alvarado-Zacarias**, N. K. Fontaine, H. Chen, R. Ryf, F. Poletti, J. R. Hayes, J. Antonio-Lopez, R. Amezcua-Correa, and G. Li, "10-mode photonic lanterns using low-index micro-structured drilling preforms," in *Optical Fiber Communication Conference*, p. Tu3J.5, Optical Society of America, 2017.

[JC81] Z. S. Eznaveh, N. K. Fontaine, H. Chen, J. E. A. Lopez, **J. C. Alvarado Zacarias**, B. Huang, A. A. Correa, C. Gonnet, P. Sillard, G. Li, A. Schülzgen, R. Ryf, and R. A. Correa, "Ultra-low dmg multimode edfa," in *2017 Optical Fiber Communications Conference and Exhibition (OFC)*, pp. 1–3, March 2017.

69

[JC82] J. J. A. van Weerdenburg, A. Alvarado, **J. C. A. Zacarias**, J. E. A. Lopez, J. H. Bonarius, D. Molin, M. Bigot-Astruc, A. M. J. Koonen, A. A. Correa, P. Sillard, R. A. Correa, and C. M. Okonkwo, "Spatial pulse position modulation for multi-mode transmission systems," in *2017 Optical Fiber Communications Conference and Exhibition (OFC)*, pp. 1–3, March 2017.

[JC83] **J. C. Alvarado-Zacarias**, B. Huang, Z. S. Eznaveh, N. K. Fontaine, H. Chen, R. Ryf, J. E. Antonio-Lopez, and R. A. Correa, "Experimental analysis of the modal evolution in photonic lanterns," in *2017 Optical Fiber Communications Conference and Exhibition (OFC)*, pp. 1–3, March 2017.

[JC84] J. E. Antonio-Lopez, S. Habib, A. Van Newkirk, G. Lopez-Galmiche, Z. S. Eznaveh, **J. C. Alvarado-Zacarias**, O. Bang, M. Bache, A. Schülzgen, and R. A. Correa, "Antiresonant hollow core fiber with seven nested capillaries," in *2016 IEEE Photonics Conference (IPC)*, pp. 402–403, Oct 2016.

[JC85] R. Ryf, H. Chen, N. K. Fontaine, A. M. Velazquez-Benitez, J. Antonio-Lopez, **J. C. Alvarado**, Z. Sanjabi Eznaveh, C. Jin, B. Huang, S. H. Chang, B. Ercan, C. Gonnet, M. Bigot-Astruc, D. Molin, F. Achten, P. Sillard, and R. Amezcua-Correa, "10-mode mode-multiplexed transmission with inline amplification," in *ECOC 2016; 42nd European Conference on Optical Communication*, pp. 1–3, Sep. 2016.

[JC86] R. Ryf, **J. C. Alvarado**, B. Huang, J. Antonio-Lopez, S. H. Chang, N. K. Fontaine, H. Chen, R. Essiambre, E. Burrows, R. Amezcua-Correa, T. Hayashi, Y. Tamura, T. Hasegawa, and T. Taru, "Long-distance transmission over coupled-core multicore fiber," in *ECOC 2016 - Post Deadline Paper; 42nd European Conference on Optical Communication*, pp. 1–3, Sep. 2016.

[JC87] N. Wang, J. E. Antonio-Lopez, **J. C. Alvarado Zacarias**, Z. Sanjabi Eznaveh, H. Wen, P. Sillard, S. Leon-Saval, A. Schulzgen, R. Amezcua-Correa, and G. Li, "Mode-selective fiber laser using a photonic lantern," in *ECOC 2016; 42nd European Conference on Optical Communication*, pp. 1–3, Sep. 2016.

[JC88] J. v. Weerdenburg, J. Antonio-Lopez, **J. Alvarado-Zacarias**, D. Molin, M. Bigot-Astruc, R. v. Uden, H. d. Waardt, T. Koonen, R. Amezcua-Correa, P. Sillard, and C. Okonkwo, "Exploiting selective excitation of strongly coupled modes to reduce dmgd in multi-mode transmission systems," in *ECOC 2016; 42nd European Conference on Optical Communication*, pp. 1–3, Sep. 2016.

[JC89] S. Wittek, R. B. Ramirez, **J. Alvarado Zacarias**, Z. S. Eznaveh, G. L. Galmiche, J. Bradford, J. Antonio-Lopez, L. Shah, and R. A. Correa, "High-power mode-selective amplification in large mode area ytterbium-doped fiber using a photonic lantern," in *Conference on Lasers and Electro-Optics*, p. SM2Q.3, Optical Society of America, 2016.

[JC90] S. Wittek, R. B. Ramirez, **J. Alvarado Zacarias**, Z. S. Eznaveh, J. Bradford, G. L. Galmiche, D. Zhang, W. Zhu, J. Antonio-Lopez, L. Shah, and R. A. Correa, "Mode-selective amplification in a large mode area yb-doped fiber using a photonic lantern," *Opt. Lett.*, vol. 41, pp. 2157–2160, May 2016.

[JC91] N. K. Fontaine, B. Huang, Z. S. Eznaveh, H. Chen, J. Cang, B. Ercan, A. Veláquez-Benitez, S. H. Chang, R. Ryf, A. Schulzgen, **Juan Carlos Alvarado Zacarias**, P. Sillard, C. Gonnet, J. E. A. Lopez, and R. Amezcua-Correa, "Multi-mode optical fiber amplifier supporting over 10 spatial modes," in *Optical Fiber Communication Conference Postdeadline Papers*, p. Th5A.4, Optical Society of America, 2016.

[JC92] A. M. Velázquez-Benítez, J. E. Antonio-López, **J. C. Alvarado-Zacarías**, G. Lopez-Galmiche, P. Sillard, D. Van Ras, C. Okonkwo, H. Chen, R. Ryf, N. K. Fontaine,

and R. Amezcua-Correa, "Scaling the fabrication of higher order photonic lanterns using microstructured preforms," in *2015 European Conference on Optical Communication (ECOC)*, pp. 1–3, Sep. 2015.

[JC93] A. M. Velazquez-Benitez, **J. C. Alvarado**, G. Lopez-Galmiche, J. E. Antonio-Lopez, J. Hernández-Cordero, J. Sanchez-Mondragon, P. Sillard, C. M. Okonkwo, and R. Amezcua-Correa, "Six mode selective fiber optic spatial multiplexer," *Opt. Lett.*, vol. 40, pp. 1663–1666, Apr 2015.

LIST OF REFERENCES

[1] *Optical Fibers*, ch. 2, pp. 24–78. John Wiley Sons, Ltd, 2010.

[2] J. D. Love, W. M. Henry, W. J. Stewart, R. J. Black, S. Lacroix, and F. Gonthier, "Tapered single-mode fibres and devices. i. adiabaticity criteria," *IEE Proceedings J - Optoelectronics*, vol. 138, no. 5, pp. 343–354, 1991.

[3] Y. Amma, Y. Sasaki, K. Takenaga, S. Matsuo, J. Tu, K. Saitoh, M. Koshiba, T. Morioka, and Y. Miyamoto, "High-density multicore fiber with heterogeneous core arrangement," in *2015 Optical Fiber Communications Conference and Exhibition (OFC)*, pp. 1–3, March 2015.

[4] K. S. Abedin, T. F. Taunay, M. Fishteyn, D. J. DiGiovanni, V. Supradeepa, J. M. Fini, M. F. Yan, B. Zhu, E. M. Monberg, and F. Dimarcello, "Cladding-pumped erbium-doped multicore fiber amplifier," *Opt. Express*, vol. 20, pp. 20191–20200, Aug 2012.

[5] M. Yamada, K. Tsujikawa, L. Ma, K. Ichii, S. Matsuo, N. Hanzawa, and H. Ono, "Optical fiber amplifier employing a bundle of reduced cladding erbium-doped fibers," *IEEE Photonics Technology Letters*, vol. 24, no. 21, pp. 1910–1913, 2012.

[6] S. Jain, T. Mizuno, Y. Jung, Q. Kang, J. R. Hayes, M. N. Petrovich, G. Bai, H. Ono, K. Shibahara, A. Sano, A. Isoda, Y. Miyamoto, Y. Sasaki, Y. Amma, K. Takenaga, K. Aikawa, C. Castro, K. Pulverer, M. Nooruzzaman, T. Morioka, S. Alam, and D. J. Richardson, "32-core inline multicore fiber amplifier for dense space division multiplexed transmissionsystems," in *ECOC 2016 - Post Deadline Paper; 42nd European Conference on Optical Communication*, pp. 1–3, 2016.

[7] R. Ryf, S. Randel, A. H. Gnauck, C. Bolle, A. Sierra, S. Mumtaz, M. Esmaeelpour, E. C. Burrows, R. Essiambre, P. J. Winzer, D. W. Peckham, A. H. McCurdy, and R. Lingle, "Mode-

division multiplexing over 96 km of few-mode fiber using coherent 6 ×6 mimo processing," *Journal of Lightwave Technology*, vol. 30, no. 4, pp. 521–531, 2012.

[8] P. Sillard, D. Molin, M. Bigot-Astruc, A. Amezcua-Correa, K. de Jongh, and F. Achten, "50 μm multimode fibers for mode division multiplexing," *J. Lightwave Technol.*, vol. 34, pp. 1672–1677, Apr 2016.

[9] J. Sakaguchi, W. Klaus, J. M. Delgado Mendinueta, B. J. Puttnam, R. S. Luís, Y. Awaji, N. Wada, T. Hayashi, T. Nakanishi, T. Watanabe, Y. Kokubun, T. Takahata, and T. Kobayashi, "Large spatial channel (36-core × 3 mode) heterogeneous few-mode multicore fiber," *Journal of Lightwave Technology*, vol. 34, pp. 93–103, Jan 2016.

[10] D. J. Richardson, J. M. Fini, and L. E. Nelson, "Space-division multiplexing in optical fibres," *Nature Photonics*, vol. 7, no. 5, pp. 354–362, 2013.

[11] P. J. Winzer, "Optical networking beyond wdm," *IEEE Photonics Journal*, vol. 4, pp. 647–651, April 2012.

[12] S. G. Leon-Saval, N. K. Fontaine, J. R. Salazar-Gil, B. Ercan, R. Ryf, and J. Bland-Hawthorn, "Mode-selective photonic lanterns for space-division multiplexing," *Opt. Express*, vol. 22, pp. 1036–1044, Jan 2014.

[13] Z. S. Eznaveh, J. E. Antonio-Lopez, J. C. A. Zacarias, A. Schülzgen, C. M. Okonkwo, and R. A. Correa, "All-fiber few-mode multicore photonic lantern mode multiplexer," *Opt. Express*, vol. 25, pp. 16701–16707, Jul 2017.

[14] A. M. Velazquez-Benitez, J. C. Alvarado, G. Lopez-Galmiche, J. E. Antonio-Lopez, J. Hernández-Cordero, J. Sanchez-Mondragon, P. Sillard, C. M. Okonkwo, and R. Amezcua-Correa, "Six mode selective fiber optic spatial multiplexer," *Opt. Lett.*, vol. 40, pp. 1663–1666, Apr 2015.

[15] A. M. Velázquez-Benítez, J. E. Antonio-López, J. C. Alvarado-Zacarías, N. K. Fontaine, R. Ryf, H. Chen, J. Hernández-Cordero, P. Sillard, C. Okonkwo, S. G. Leon-Saval, *et al.*, "Scaling photonic lanterns for space-division multiplexing," *Scientific reports*, vol. 8, no. 1, p. 8897, 2018.

[16] K. Igarashi, D. Souma, K. Takeshima, and T. Tsuritani, "Selective mode multiplexer based on phase plates and mach-zehnder interferometer with image inversion function," *Opt. Express*, vol. 23, pp. 183–194, Jan 2015.

[17] N. K. Fontaine, R. Ryf, H. Chen, D. T. Neilson, K. Kim, and J. Carpenter, "Laguerre-gaussian mode sorter," *Nature communications*, vol. 10, no. 1, p. 1865, 2019.

[18] N. K. Fontaine, R. Ryf, H. Chen, D. Neilson, and J. Carpenter, "Design of high order mode-multiplexers using multiplane light conversion," in *2017 European Conference on Optical Communication (ECOC)*, pp. 1–3, Sep. 2017.

[19] G. Labroille, B. Denolle, P. Jian, P. Genevaux, N. Treps, and J.-F. Morizur, "Efficient and mode selective spatial mode multiplexer based on multi-plane light conversion," *Opt. Express*, vol. 22, pp. 15599–15607, Jun 2014.

[20] B. Guan, B. Ercan, N. K. Fontaine, R. P. Scott, and S. J. B. Yoo, "Mode-group-selective photonic lantern based on integrated 3d devices fabricated by ultrafast laser inscription," in *Optical Fiber Communication Conference*, p. W2A.16, Optical Society of America, 2015.

[21] R. Ryf, N. K. Fontaine, M. A. Mestre, S. Randel, X. Palou, C. Bolle, A. H. Gnauck, S. Chandrasekhar, X. Liu, B. Guan, R.-J. Essiambre, P. J. Winzer, S. G. Leon-Saval, J. Bland-Hawthorn, R. Delbue, P. Pupalaikis, A. Sureka, Y. Sun, L. Grüner-Nielsen, R. V. Jensen, and R. Lingle, "12 × 12 mimo transmission over 130-km few-mode fiber," in *Frontiers in Optics 2012/Laser Science XXVIII*, p. FW6C.4, Optical Society of America, 2012.

[22] R. Ryf, H. Chen, N. K. Fontaine, A. M. Velázquez-Benítez, J. Antonio-López, C. Jin, B. Huang, M. Bigot-Astruc, D. Molin, F. Achten, P. Sillard, and R. Amezcua-Correa, "10-mode mode-multiplexed transmission over 125-km single-span multimode fiber," in *2015 European Conference on Optical Communication (ECOC)*, pp. 1–3, Sep. 2015.

[23] R. Ryf, N. K. Fontaine, B. Guan, B. Huang, M. Esmaeelpour, S. Randel, A. H. Gnauck, S. Chandrasekhar, A. Adamiecki, G. Raybon, R. W. Tkach, R. Shubochkin, Y. Sun, and R. Lingle, "305-km combined wavelength and mode-multiplexed transmission over conventional graded-index multimode fibre," in *2014 The European Conference on Optical Communication (ECOC)*, pp. 1–3, Sep. 2014.

[24] J. van Weerdenburg, A. Velàzquez-Benitez, R. van Uden, P. Sillard, D. Molin, A. Amezcua-Correa, E. Antonio-Lopez, M. Kuschnerov, F. Huijskens, H. de Waardt, T. Koonen, R. Amezcua-Correa, and C. Okonkwo, "10 spatial mode transmission using low differential mode delay 6-lp fiber using all-fiber photonic lanterns," *Opt. Express*, vol. 23, pp. 24759–24769, Sep 2015.

[25] J. van Weerdenburg, R. Ryf, J. C. Alvarado-Zacarias, R. A. Alvarez-Aguirre, N. K. Fontaine, H. Chen, R. Amezcua-Correa, Y. Sun, L. Grüner-Nielsen, R. V. Jensen, R. Lingle, T. Koonen, and C. Okonkwo, "138-tb/s mode- and wavelength-multiplexed transmission over six-mode graded-index fiber," *J. Lightwave Technol.*, vol. 36, pp. 1369–1374, Mar 2018.

[26] N. K. Fontaine, R. Ryf, M. A. Mestre, B. Guan, X. Palou, S. Randel, Y. Sun, L. Grüner-Nielsen, R. V. Jensen, and R. Lingle, "Characterization of space-division multiplexing systems using a swept-wavelength interferometer," in *Optical Fiber Communication Conference/National Fiber Optic Engineers Conference 2013*, p. OW1K.2, Optical Society of America, 2013.

[27] J. Tu, K. Saitoh, M. Koshiba, K. Takenaga, and S. Matsuo, "Design and analysis of large-effective-area heterogeneous trench-assisted multi-core fiber," *Opt. Express*, vol. 20, pp. 15157–15170, Jul 2012.

[28] T. Hayashi, T. Taru, O. Shimakawa, T. Sasaki, and E. Sasaoka, "Design and fabrication of ultra-low crosstalk and low-loss multi-core fiber," *Opt. Express*, vol. 19, pp. 16576–16592, Aug 2011.

[29] S. Matsuo, K. Takenaga, Y. Sasaki, Y. Amma, S. Saito, K. Saitoh, T. Matsui, K. Nakajima, T. Mizuno, H. Takara, Y. Miyamoto, and T. Morioka, "High-spatial-multiplicity multicore fibers for future dense space-division-multiplexing systems," *Journal of Lightwave Technology*, vol. 34, pp. 1464–1475, March 2016.

[30] K. Saitoh and S. Matsuo, "Multicore fiber technology," *J. Lightwave Technol.*, vol. 34, pp. 55–66, Jan 2016.

[31] T. Hayashi, R. Ryf, N. K. Fontaine, C. Xia, S. Randel, R. Essiambre, P. J. Winzer, and T. Sasaki, "Coupled-core multi-core fibers: High-spatial-density optical transmission fibers with low differential modal properties," in *2015 European Conference on Optical Communication (ECOC)*, pp. 1–3, Sep. 2015.

[32] H. Chen, N. K. Fontaine, R. Ryf, R. Essiambre, L. Wang, Y. Messaddeq, S. LaRochelle, T. Hayashi, T. Nagashima, and T. Sasaki, "Transmission over coupled six-core fiber with two in-line cladding-pumped six-core edfas," in *2015 European Conference on Optical Communication (ECOC)*, pp. 1–3, Sep. 2015.

[33] N. K. Fontaine, J. E. A. Lopez, H. Chen, R. Ryf, D. Neilson, A. Schulzgen, J. C. A. Zaharias, R.-J. Essiambre, H. Sakuma, T. Hasegawa, T. Nakanishi, T. Hayashi, and R. Amezcua-Correa, "Coupled-core optical amplifier," in *Optical Fiber Communication Conference Post-deadline Papers*, p. Th5D.3, Optical Society of America, 2017.

[34] M. Yoshida, T. Hirooka, and M. Nakazawa, "Fused type fan-out device for multi-core fiber based on bundled structure," in *2016 Optical Fiber Communications Conference and Exhibition (OFC)*, pp. 1–3, March 2016.

[35] K. Watanabe, T. Saito, K. Imamura, and M. Shiino, "Development of fiber bundle type fan-out for multicore fiber," in *2012 17th Opto-Electronics and Communications Conference*, pp. 475–476, July 2012.

[36] K. Watanabe, T. Saito, and M. Shiino, "Development of fiber bundle type fan-out for 19-core multicore fiber," in *2014 OptoElectronics and Communication Conference and Australian Conference on Optical Fibre Technology*, pp. 44–46, July 2014.

[37] T. Watanabe, M. Hikita, and Y. Kokubun, "Laminated polymer waveguide fan-out device for uncoupled multi-core fibers," *Opt. Express*, vol. 20, pp. 26317–26325, Nov 2012.

[38] T. Watanabe, M. Hikita, and Y. Kokubun, "19-core fan-in/fan-out waveguide device for dense uncoupled multi-core fiber," in *2013 IEEE Photonics Conference*, pp. 303–304, Sep. 2013.

[39] J. Sakaguchi, W. Klaus, B. J. Puttnam, J. M. D. Mendinueta, Y. Awaji, N. Wada, Y. Tsuchida, K. Maeda, M. Tadakuma, K. Imamura, R. Sugizaki, T. Kobayashi, Y. Tottori, M. Watanabe, and R. V. Jensen, "19-core mcf transmission system using edfa with shared core pumping coupled via free-space optics," *Opt. Express*, vol. 22, pp. 90–95, Jan 2014.

[40] P. Sillard, M. Bigot-Astruc, D. Boivin, H. Maerten, and L. Provost, "Few-mode fiber for uncoupled mode-division multiplexing transmissions," in *2011 37th European Conference and Exhibition on Optical Communication*, pp. 1–3, Sep. 2011.

[41] P. Sillard, D. Molin, M. Bigot-Astruc, K. De Jongh, F. Achten, A. M. Velázquez-Benítez, R. Amezcua-Correa, and C. M. Okonkwo, "Low-differential-mode-group-delay 9-lp-mode fiber," *Journal of Lightwave Technology*, vol. 34, pp. 425–430, Jan 2016.

[42] R. Ryf, J. C. Alvarado, B. Huang, J. Antonio-Lopez, S. H. Chang, N. K. Fontaine, H. Chen, R. Essiambre, E. Burrows, R. Amezcua-Correa, T. Hayashi, Y. Tamura, T. Hasegawa, and T. Taru, "Long-distance transmission over coupled-core multicore fiber," *ECOC PDP*, Sep. 2016.

[43] R. Ryf, J. C. Alvarado-Zacarias, S. Wittek, N. K. Fontaine, R.-J. Essiambre, H. Chen, R. Amezcua-Correa, H. Sakuma, T. Hayashi, and T. Hasegawa, "Coupled-core transmission over 7-core fiber," in *Optical Fiber Communication Conference Postdeadline Papers 2019*, p. Th4B.3, Optical Society of America, 2019.

[44] T. Hayashi, Y. Tamura, T. Hasegawa, and T. Taru, "Record-low spatial mode dispersion and ultra-low loss coupled multi-core fiber for ultra-long-haul transmission," *J. Lightwave Technol.*, vol. 35, pp. 450–457, Feb 2017.

[45] R. Ryf, N. K. Fontaine, S. Wittek, K. Choutagunta, M. Mazur, H. Chen, J. Carlos Alvarado-Zacarias, R. Amezcua-Correa, M. Capuzzo, R. Kopf, A. Tate, H. Safar, C. Bolle, D. T. Neilson, E. Burrows, K. Kim, M. Bigot-Astruc, F. Achten, P. Sillard, A. Amezcua-Correa, J. M. Kahn, J. Schröder, and J. Carpenter, "High-spectral-efficiency mode-multiplexed transmission over graded-index multimode fiber," in *2018 European Conference on Optical Communication (ECOC)*, pp. 1–3, Sep. 2018.

[46] S. Mumtaz, R. Essiambre, and G. P. Agrawal, "Reduction of nonlinear impairments in coupled-core multicore optical fibers," in *2012 IEEE Photonics Society Summer Topical Meeting Series*, pp. 175–176, July 2012.

[47] M. Wada, T. Sakamoto, S. Aozasa, T. Yamamoto, and K. Nakajima, "L-band randomly-coupled 12 core erbium doped fiber amplifier," in *2019 Optical Fiber Communications Conference and Exhibition (OFC)*, pp. 1–3, March 2019.

[48] T. Ohtsuka, M. Tanaka, H. Sakuma, T. Hasegawa, T. Hayashi, and H. Tazawa, "Coupled 7-core erbium doped fiber amplifier and its characterization," in *Optical Fiber Communication Conference (OFC) 2019*, p. W2A.19, Optical Society of America, 2019.

[49] J. C. Alvarado-Zacarias, C. Matte-Breton, R. Ryf, N. K. Fontaine, H. Chen, S. Wittek, H. Sakuma, T. Ohtsuka, T. Hayashi, T. Hasegawa, S. LaRochelle, and R. Amezcua-Correa, "Characterization of coupled-core fiber amplifiers using swept-wavelength interferometer," in *Optical Fiber Communication Conference (OFC) 2019*, p. Th1B.6, Optical Society of America, 2019.

[50] N. K. Fontaine, B. Huang, Z. S. Eznaveh, H. Chen, J. Cang, B. Ercan, A. Veláquez-Benitez, S. H. Chang, R. Ryf, A. Schulzgen, J. C. A. Zaharias, P. Sillard, C. Gonnet, J. E. A. Lopez, and R. Amezcua-Correa, "Multi-mode optical fiber amplifier supporting over 10 spatial modes," in *Optical Fiber Communication Conference Postdeadline Papers*, p. Th5A.4, Optical Society of America, 2016.

[51] N. K. Fontaine, "Characterization of space-division multiplexing fibers using swept-wavelength interferometry," in *Optical Fiber Communication Conference*, p. W4I.7, Optical Society of America, 2015.

[52] M. Mazur, N. K. Fontaine, R. Ryf, H. Chen, D. T. Neilson, M. Bigot-Astruc, F. Achten, P. Sillard, A. Amezcua-Correa, J. Schröder, and J. Carpenter, "Characterization of long multi-mode fiber links using digital holography," in *Optical Fiber Communication Conference (OFC) 2019*, p. W4C.5, Optical Society of America, 2019.

[53] N. K. Fontaine, R. Ryf, H. Chen, S. Wittek, J. Li, J. C. Alvarado, J. E. A. Lopez, M. Cappuzzo, R. Kopf, A. Tate, H. Safar, C. Bolle, D. T. Neilson, E. Burrows, K. W. Kim, P. Sillard, F. Achten, M. Bigot, A. Amezcua-Correa, R. A. Correa, J. Du, Z. He, and J. Carpenter, "Pack-

aged 45-mode multiplexers for a $50 - \mu$m graded index fiber," in *2018 European Conference on Optical Communication (ECOC)*, pp. 1–3, 2018.